The adhesion G protein-coupled receptor GPR56/ADGRG1 is an inhibitory receptor on human NK cells

Gin-Wen Chang[1,10], Cheng-Chih Hsiao[2,10], Yen-Ming Peng[1], Felipe A. Vieira Braga[3], Natasja A.M. Kragten[3], Ester B. M. Remmerswaal[2,4], Martijn D. B. van de Garde[2], Rachel Straussberg[5], Gabriele M. König[6], Evi Kostenis[6], Vera Knäuper[7], Linde Meyaard[8], René A.W. van Lier[3], Klaas P.J.M. van Gisbergen[3], Hsi-Hsien Lin[1,9,11,*], and Jörg Hamann[2,11,*]

[1]Graduate Institute of Biomedical Sciences, College of Medicine, Chang Gung University, 333 Tao-Yuan, Taiwan; [2]Department of Experimental Immunology and [4]Renal Transplant Unit, Academic Medical Center, University of Amsterdam, 1105 AZ Amsterdam, The Netherlands; [3]Department of Hematopoiesis, Sanquin Research and Landsteiner Laboratory, Academic Medical Center, University of Amsterdam, 1066 CX Amsterdam, The Netherlands; [5]Department of Child Neurology, Neurogenetics Clinic, Schneider Children's Medical Center, Petach Tikva and Sackler Faculty of Medicine, Tel Aviv University, Tel Aviv 69978, Israel; [6]Institute for Pharmaceutical Biology, University of Bonn, 53115 Bonn, Germany; [7]Dental School, Cardiff University, Cardiff CF14 4XN, United Kingdom; [8]Department of Immunology, University Medical Center Utrecht, 3584 EA Utrecht, The Netherlands; [9]Chang Gung Immunology Consortium and Department of Anatomic Pathology, Chang Gung Memorial Hospital-Linkou, 333 Tao-Yuan, Taiwan. [10]Co-first author, [11]Co-senior author

Running title: GPR56 regulates NK-cell cytotoxicity

Keywords: adhesion GPCRs / cytotoxicity / immune regulation / NK cells / transcription factor

Manuscript length: 26 pages, 64,985 characters, 64 references, and 5 figures

***Correspondence:** Dr. Jörg Hamann, Department of Experimental Immunology, K0-144, Academic Medical Center, University of Amsterdam, Meibergdreef 9, 1105 AZ Amsterdam, The Netherlands. E-mail: j.hamann@amc.uva.nl and Dr. Hsi-Hsien Lin, Department of Microbiology and Immunology, College of Medicine, Chang Gung University, 259 Wen-Hwa 1st Road, Kwei-Shan, 333 Tao-Yuan, Taiwan. E-mail: hhlin@mail.cgu.edu.tw

SUMMARY

Natural killer (NK) cells possess potent cytotoxic mechanisms that need to be tightly controlled. We here explored the regulation and function of GPR56/ADGRG1, an adhesion G protein-coupled receptor implicated in developmental processes and expressed distinctively in mature NK cells. Expression of GPR56 was triggered by Hobit, a homolog of Blimp-1, and declined upon cell activation. Through studying NK cells from polymicrogyria patients with disease-causing mutations in the *ADGRG1* gene, encoding GPR56, and NK-92 cells ectopically expressing the receptor, we found that GPR56 negatively regulates immediate effector functions, including production of inflammatory cytokines and cytolytic proteins, degranulation, and target cell killing. GPR56 pursues this activity by associating with the tetraspanin CD81. We conclude that GPR56 inhibits natural cytotoxicity of human NK cells.

INTRODUCTION

Natural killer (NK) cells are innate lymphoid cells that develop, mainly in the bone marrow, through a series of distinct phenotypic stages before they enter the circulation to specifically eradicate virus-infected and transformed cells (Freud and Caligiuri, 2006). Upon target cell encounter, differentiated $CD56^{dim}$ NK cells produce large amounts of cytokines, chemokines, and cytolytic proteins, similar to effector-type $CD8^+$ T cells (Fauriat et al., 2010; Nagler et al., 1989; Vivier et al., 2008). The activity of cytotoxic $CD56^{dim}$ NK and $CD8^+$ T cells is regulated by a comprehensive repertoire of activating and inhibitory receptors, including immunoglobulin-like receptors and C-type lectins (Lanier, 2008; Pegram et al., 2011).

G protein-coupled receptors (GPCRs) guide numerous cellular processes, including development and differentiation (Pierce et al., 2002), yet, in the immune system, they have been linked primarily with chemotaxis (Walzer and Vivier, 2011). Others and we recently showed that human cytotoxic lymphocytes, including $CD56^{dim}$ NK cells and $CD27^-CD45RA^+$ T cells, express the adhesion family GPCR (aGPCR) GPR56/ADGRG1 (Chiesa et al., 2010; Peng et al., 2011). Expression of GPR56 correlated closely with production of the cytolytic proteins perforin, granzyme A, and granzyme B and was not found in non-cytotoxic lymphocytes or myeloid cells.

aGPCRs possess an N-terminal fragment (NTF) and a C-terminal fragment (CTF) that arise from autocatalytic cleavage at a GPCR-proteolytic site (GPS), embedded in a juxtamembranous GPCR autoproteolysis-inducing (GAIN) domain (Araç et al., 2012; Lin et al., 2004). At the cell surface, the NTF remains non-covalently attached to the CTF, giving rise to a characteristic bipartite structure with the two fragments being engaged in distinct activities (Langenhan et al., 2013). The NTF of GPR56 binds transglutaminase and collagen III, while the CTF recruits $G\alpha$ proteins leading to activation of RhoA (Ras homolog gene family member A) and mTOR (mechanistic target of rapamycin) pathways (Ackerman et al., 2015; Giera et al., 2015; Iguchi et al., 2008; Little et al., 2004; Luo et al., 2011; Paavola et al., 2011; Stoveken et al., 2015; White et al., 2014; Xu et al., 2006).

We here tested the relation of GPR56 with the differentiation, activation, and function of human NK cells. We provide evidence that GPR56 expression is triggered by the transcriptional repressor Hobit (homolog of Blimp-1 in T cells), is downregulated upon cellular activation, and inhibits immediate effector functions, including inflammatory cytokine and cytolytic protein production, degranulation, and target cell killing. We conclude that GPR56 is a differentiation marker and inhibitory receptor on human NK cells.

RESULTS

Hobit, the human homolog of Blimp-1 in T cells, drives expression of GPR56 in non-dividing, fully differentiated human NK cells

GPR56 is expressed by all human cytotoxic lymphocytes, including $CD56^{dim}$ NK cells (Chiesa et al., 2010; Peng et al., 2011). Upon stimulation with common gamma chain cytokines, such as interleukin (IL)-2, proliferating NK cells lose expression of GPR56 (Chiesa et al., 2010) (Figure 1A). IL-2-dependent cytotoxic NK-92 cells weakly express GPR56. IL-2 withdrawal stopped NK-92 cell division, leading to cell cycle arrest in the G1 phase and surface expression of GPR56 (Figure 1B). Of note, IL-2 deprivation caused upregulation of surface markers commonly associated with terminal cell differentiation, such as KLRG1 (killer cell lectin-like receptor subfamily G member 1) and B3GAT1 (galactosylgalactosylxylosylprotein 3-beta-glucuronosyltransferase 1), the enzyme that generates the CD57 glycosylation epitope, and downregulation of the cell exhaustion marker PD1 (programmed cell death 1) (Figure 1C). These changes correlated with altered expression of transcription factors involved in effector lymphocyte development, such as Blimp-1 (B lymphocyte-induced maturation protein-1), Bcl-6 (B-cell lymphoma 6), T-bet (T-box expressed in T cells), Eomes (eomesodermin), and the recently identified Hobit (homolog of Blimp-1 in T cells) (van Gisbergen et al., 2012; Vieira Braga et al., 2015) (Figure 1C). In line with their in part contrary activities (Crotty et al., 2010; Daussy et al., 2014; Knox et al., 2014), downregulation of Blimp-1 and T-bet was accompanied by upregulation of Bcl-6 and Eomes, respectively. The most prominent change, with a ~25-fold induction, occurred with Hobit.

We next correlated GPR56 protein expression with the presence of various surface molecules, cytolytic proteins, and transcription factors in primary NK cells. In line with its absence on immature $CD56^{high}$ NK cells, we detected almost no GPR56 on NK cells from tonsil (data not shown). In contrast, mature circulating NK cells commonly expressed GPR56. GPR56 was acquired prior to the late differentiation/senescence markers KLRG1 and CD57 (Björkström et al., 2010; Lopez-Vergès et al., 2010), as most clearly exemplified by cells from cord blood (Figure 1D). In line with the uniform presence of GPR56 on $CD56^{dim}$ NK cells, no association was found with the expression of activating or inhibitory natural cytotoxicity receptors (NKp30, NKp44, NKp46), NK-cell receptors (NKG2a, NKG2c, NKG2d), and killer immunoglobulin-like receptors (KIR2DL1/S1, KIR2DL2/L3, KIR3DL1) (Figure S1). Supporting previous findings (Peng et al., 2011), the presence of GPR56 correlated with production of the cytolytic mediators perforin and granzyme B (Figure S1). Cells expressing GPR56 were positive for the transcription factors T-bet, Eomes, and Hobit; in particular, expression of GPR56 and Hobit was strongly associated

(Figure 1D). Thus, non-dividing, fully differentiated NK cells, found in the circulation and commonly identified as $CD56^{dim}$ cells, express GPR56 in a distinctive manner.

Recent studies identified a subset of long-lived memory-like NK cells, associated with prior human cytomegalovirus infection, that can mount long-term effective recall responses (Lee et al., 2015; Schlums et al., 2015; Zhang et al., 2013). We found that these memory-like NK cells, which can be distinguished by low expression of the transcription factor PLZF (promyelocytic leukemia zinc finger) and lack of FcRγ (high-affinity IgE receptor, γ subunit), express GPR56 (Figure 1E).

The T-box transcription factor Eomes is crucially involved in effector lymphocyte differentiation and, like GPR56, is expressed in differentiating neurons in the developing human brain (Elsen et al., 2013). Intriguingly, lack of Eomes causes a microcephaly syndrome (Baala et al., 2007) similar to the malformation seen in patients with null GPR56 expression (Piao et al., 2004). To test a causal relationship between Eomes and the expression of GPR56, we applied shRNA knockdown of *EOMES* in NK-92 cells. Reduced Eomes expression did not prevent GPR56 induction upon IL-2 withdrawal (Figure 1F). In contrast, knockdown of *ZNF683*, encoding Hobit, largely prevented GPR56 induction in NK-92 cells cultured without IL-2 (Figure 1F-H). Furthermore, ectopic expression of Hobit in Jurkat cells, which express neither GPR56 nor Hobit, induced expression of GPR56 (Figure 1I-K), indicating that Hobit drives the expression of GPR56 in human lymphocytes.

GPR56 deficiency does not affect NK-cell development but correlates with elevated NK-cell functions

Loss-of-function mutations in *ADGRG1*, encoding GPR56, cause a severe cortical malformation, known as bilateral frontoparietal polymicrogyria (BFPP) (Piao et al., 2004; 2005). To test whether defective expression of GPR56 would affect NK-cell differentiation and/or function, we studied two unrelated pairs of BFPP siblings bearing the mutations 1693C>T (R565W) and 1036T>A (C346S), respectively. Previous in vitro-analysis revealed that both mutations strongly reduce surface expression of GPR56 (Chiang et al., 2011; Jin et al., 2007). We found that the R565W mutation abolished GPR56 expression on NK (and T) cells completely, whereas the C346S mutation reduced surface levels of GPR56 by about 20-fold (Figure 2A and Figure S2). All patients had normal numbers of circulating NK cells (Figure 2A and Figure S2C). Moreover, their NK cells had a fairly normal phenotype, based on the expression of surface molecules, including receptors with activating or inhibiting effector functions, cytolytic proteins, and transcription factors (Figure 2A and Figure S2). However, $CD56^{dim}$ NK cells in the R565W patients, which

completely lacked GPR56, expressed lower levels of CD94, indicating maturation. Moreover, the cells expressed less/no inhibitory KIR2DL1/S1, probably due to allelic variation, while steady-state expression of cytolytic proteins was unchanged (granzyme B) or marginally reduced (perforin).

The phenotypic changes found in $CD56^{dim}$ NK cells in the 1693C>T (R565W) siblings raised the possibility that the cytolytic capacity of NK cells in these patients was altered. Indeed, their NK cells killed K562 cells more efficiently than control cells, as indicated by enhanced degranulation (CD107a expression) and induction of apoptosis in the target cells. In addition, target cell contacts resulted in enhanced production of tumor necrosis factor (TNF) and interferon (IFN)γ by GPR56-deficient NK cells (Figure 2B,C). Thus, lack of GPR56 did not hamper normal NK-cell development, but appeared to enhance their functional capacity.

NK cells downregulate GPR56 upon cytokine stimulation

Upon encounter of virus-infected or transformed cells, NK cells downregulate inhibitory receptors to acquire maximal killing capacity (Pegram et al., 2011). PMA (phorbol-12-myristate-13-acetate) stimulation downregulates ectopic GPR56 in monocytic U937 cells (Little et al., 2004). In primary NK cells, PMA treatment resulted in loss of GPR56 at concentrations as low as 1 ng/ml, which was enhanced by ionomycin (data not shown, Figure 3A, and Figure S3A). With a loss of >60% of cell surface GPR56 within 10 min and >80% after 2 h, kinetics resembled the downregulation of CD16 (Figure 3B). Studies with pharmacological inhibitors confirmed the involvement of protein kinase (PK)C, but not MAP kinases, in PMA-induced GPR56 downregulation (Figure S3B). Activation of PKA with forskolin did not affect GPR56 surface levels (Figure S3A).

aGPCRs are downregulated by internalization or shedding (Karpus et al., 2013; Langenhan et al., 2013). The dynamin inhibitor dynasore that prevents internalization and GM6001, a broad-spectrum matrix metalloproteinase (MMP) inhibitor, synergistically blocked the downregulation of GPR56 upon PMA stimulation (Figure 3C). In contrast, downregulation of CD16 upon PMA stimulation was primarily blocked by GM6001 (Figure S3C). Cleavage of CD16 involves a disintegrin and metalloproteinase (ADAM)17, expressed in NK cells (Romee et al., 2013). Indeed, two ADAM17 inhibitors affected PMA-induced downregulation of CD16, but not GPR56 (Figure S3C). NK cells pre-incubated with fluorescently labeled anti-GPR56 or anti-CD16 monoclonal antibodies (mAbs) on ice and subsequently treated with PMA for 2 h had lost ~10% of the GPR56-bound mAb, but ~70% of the CD16-bound mAb, indicating that GPR56 was partially endocytosed from the cell surface (Figure 3D). Moreover, an increase in soluble GPR56

in the medium was detected after NK-cell stimulation with PMA, which was abrogated by inhibitors of PKC and MMPs (Figure 3E). Thus, PKC activation induces downregulation of GPR56 in primary NK cells via internalization and shedding.

Physiological activation of primary NK cells occurs through pro-inflammatory cytokines, crosslinking of activating receptors, or exposure to target cells. To test the effect of cytokines, we incubated peripheral blood mononuclear cells (PBMCs) for 12–24 h with IL-2, IL-15, or IL-18, alone or in combination. A combination of IL-15 and IL-18 reduced GPR56 surface levels by ~40% after 12 h and by ~70% after 24 h, which was more efficient as compared to the downregulation of CD16 by these cytokines (Figure 3F). Inhibition of PKC and MMPs blocked the downregulation of GPR56 and CD16, while blockade of endocytosis with dynasore had no effect (Figure 3G). In line with our former data, inhibition of ADAM17 blocked the downregulation of CD16, but not GPR56, leaving the identity of the sheddase that releases the NTF of GPR56 open (data not shown). Crosslinking CD16 or exposure to K562 had a small effect on GPR56 surface expression (data not shown). In sum, physiological NK-cell activation through cytokines causes downregulation of GPR56 by shedding of the NTF of the receptor.

Notably, activation of primary NK cells downregulates the expression of Hobit. In PBMCs stimulated for 2 h with PMA or for 12–24 h with cytokines, we found a clear decrease in Hobit and GPR56 transcript levels (Figure 3H), indicating that NK-cell activation causes downregulation of GPR56, immediately, by shedding of the NTF (see above), and permanently, by terminating gene expression.

GPR56 controls NK-cell effector functions

To further examine the role of GPR56 in NK-cell function, we applied ectopic GPR56 expression in NK-92 cells (Peng et al., 2011). Proper expression and autoproteolytic modification of the receptor were confirmed by flow cytometry and Western blot analysis, respectively (data not shown). GPR56 overexpression did not affect cell growth (data not shown). Quantification of cytolytic proteins revealed a much-reduced expression of granzyme B, both at the transcript and protein level, in NK-92–GPR56 cells (Figure 4A,B). In contrast, mRNA and protein levels of perforin were comparable between NK-92–Neo and NK-92–GPR56 cells. Moreover, a lower level of TNF but not IFNγ transcript was detected in NK-92–GPR56 cells (Figure 4C). When activated by PMA, NK-92–GPR56 cells produced less TNF and IFNγ than NK-92–Neo cells (Figure 4D,E). These results suggested that forced GPR56 expression in NK-92 cells negatively regulates the expression of effector molecules.

Hence, we examined various NK-cell effector activities, including target cell conjugation and

killing, degranulation, and cytokine production (both intracellular and secreted). GPR56 significantly attenuated cytotoxicity against K562 cells, as indicated by reduced target cell apoptosis, NK-cell degranulation, and production of TNF and IFNγ, when compared with NK-92–Neo cells (Figure 4F-H). The compromising effects of GPR56 on NK-cell cytotoxicity were also observed when NK-92–GPR56 cells were incubated with target cells more resistant to cell conjugation and killing, such as THP-1 and HeLa cells (Figure S4). Taken together, we concluded that GPR56 expression in NK-92 cells attenuates cytotoxic capacity, in accordance with the findings derived from the primary NK cells of BFPP patients.

GPR56 complexes with CD81 to negatively regulate NK-cell effector functions

aGPCRs possess a characteristic bipartite structure (Hamann et al., 2015). Notably, target cell killing was also reduced in NK-92 cells expressing cleavage-deficient GPR56, indicating that autocatalytic processing at the GPS is not a prerequisite for the inhibitory activity of GPR56 in NK cells (Figure S5). Moreover, we could not confirm interaction with collagen III, the binding partner of GPR56 on neuronal cells (Luo et al., 2011) (Figure S6). These findings are in line with reports showing that the CTF of GPR56 can signal independently of the NTF (Kishore et al., 2016; Paavola et al., 2011; Yang et al., 2011).

The CTF of GPR56 forms complexes with the tetraspanin proteins CD9 and CD81 at the cell surface (Little et al., 2004). CD81 has been previously reported to inhibit human NK-cell functions, when crosslinked by the major hepatitis C virus (HCV) envelope protein E2 or anti-CD81 mAbs (Crotta et al., 2002; Tseng and Klimpel, 2002). Flow-cytometric analysis showed significant amounts of CD81, but little CD9, in NK-92 cells. Interestingly, GPR56 overexpression strongly lowered CD81 protein levels, even though RNA transcript levels were reduced only slightly (Figure S7A), which might be explained by a relatively high turnover of GPR56 (and complexed CD81) in NK-92–GPR56 cells (data not shown). Western blotting indicated that NK-cell activation by PMA reduced GPR56 protein levels without affecting CD81, but interaction with K562 target cells diminished the levels of both GPR56 and CD81 (Figure S7B). On the other hand, no significant changes in CD81 protein levels were observed when NK-92–Neo cells were activated by PMA or by interaction with K562 cells (Figure S7B). This result suggested that NK-92–K562 cell interaction might cause dynamic changes of the GPR56–CD81 complex on the cell surface.

Indeed, confocal immunofluorescence microscopy revealed marked redistribution of GPR56 and CD81 in NK-92–GPR56 cells before and after target cell conjugation (Figure 5A). At steady state, GPR56 and CD81 were largely co-localized and distributed homogenously on the cell surface.

After conjugation with K562 cells, the levels of both GPR56 and CD81 were reduced, and the two receptors were clustered mostly to areas resembling immune synapses, where granzyme B also accumulated (Figure 5A). Such reduction and clustering of CD81 protein was not observed in NK-92–Neo cells, suggesting a critical role for GPR56 in this process.

We confirmed the formation and reduction of GPR56–CD81 complexes in NK-92–K562 co-cultures by (immunoprecipitation) IP and IP–re-IP experiments (Figure 5B). CD81 was readily detected in NK-92–GPR56 cell lysate immunoprecipitated with the anti-GPR56 CG2 mAb. Critically, the amount of precipitated CD81 was comparable in the lysate of resting and PMA-activated NK-92–GPR56 cells, but much reduced in the same cells co-cultured with K562 cells. This result was further verified by IP with the anti-CD81 mAb first, followed by re-IP with anti-GPR56 CG2 mAb (Figure 5B). These results indicated that GPR56 indeed associates with CD81 and that the GPR56–CD81 complexes are diminished upon NK-cell interaction with target cells.

To delineate how the GPR56–CD81 complex modulated NK-cell function, anti-GPR56 mAbs were employed. Crosslinking of GPR56 by mAb ligation with CG2 and CG5, but not CG3, caused a rapid dissociation of the GPR56–CD81 complex as shown by the IP experiments (Figure 5C and Figure S7C). Importantly, the cytolytic function and cytokine (TNF and IFNγ) secretion of NK-92–GPR56 and human primary NK cells were greatly enhanced in the presence of CG2 or CG5 mAbs, whereas the isotype control Ab and CG3 mAb failed to show such an effect (Figure 5D-G). Similarly, shRNA knockdown of CD81 restored K562 target cell killing by NK-92–GPR56 cells (Figure S7D-F). Finally, we tested whether $G\alpha_{q/11}$, which has been implicated in GPR56–CD81 complex signaling (Little et al., 2004), is required. Of note, a highly selective $G\alpha_{q/11/14}$ inhibitor (FR900359) (Schrage et al., 2015) did not restore cytolytic activity in NK-92–GPR56 cells (Figure S7G). We concluded that association with CD81, but not $G\alpha_{q/11}$ signaling, is crucial for the ability of GPR56 to inhibit NK-cell functions.

DISCUSSION

We here describe GPR56 as an inhibitory receptor expressed by human CD56^{dim} NK cells. CD56^{dim} NK and CD27^{-}CD45RA^{+} T cells are highly reactive cytotoxic effector lymphocytes that protect the body against harmful viruses and neoplasms. The effective cytotoxicity, displayed by these cells, requires a tight interplay between activating and inhibiting control mechanisms (Caligiuri, 2008). We previously reported that cytotoxic human lymphocytes, in contrast to non-cytotoxic lymphoid or myeloid blood cells, express GPR56 (Peng et al., 2011). This study extends these findings by showing that GPR56 is induced in CD56^{dim} NK cells prior to the upregulation of KLRG1 and CD57, which both appear at later stages of differentiation, associated with terminal differentiation (Björkström et al., 2010; Lopez-Vergès et al., 2010; Voehringer et al., 2002). Of note, long-lived memory-like NK cells, defined by absent/low expression of FcRγ and PLZF (Lee et al., 2015; Schlums et al., 2015; Zhang et al., 2013), also expressed GPR56. GPR56 seems to be the best currently available surrogate surface marker to indicate cytolytic capacity across all lymphocyte subsets.

The restricted expression of GPR56 by only CD56^{dim} NK (and CD27^{-}CD45RA^{+} T) cells indicates tight control of its induction and regulation at the transcript and protein level. We obtained evidence that expression of GPR56 is induced by Hobit, a close relative of Blimp-1, recently discovered by us (van Gisbergen et al., 2012). In humans, Hobit is expressed in quiescent effector NK and T cells, very closely matching the expression of GPR56 (Vieira Braga et al., 2015). Implying a causal relationship, Hobit knockdown in NK-92 cells prevented induction of GPR56 upon IL-2 withdrawal, and ectopic Hobit enabled GPR56 expression in Jurkat T cells. In contrast, manipulating the expression of Eomes did not affect GPR56 expression, despite its prominent role in the differentiation and maturation of effector NK and T cells and, like GPR56, its expression in developing neurons and relationship with polymicrogyria (Baala et al., 2007). Thus, on current evidence, GPR56 is a transcriptional target of Hobit in human NK and T cells.

Of note, the GPR56 locus has 17 transcriptional start sites in humans, which are targets of different transcription factors, such as peroxisome proliferator-activated receptor gamma co-activator 1-alpha 4 (PGC-1α4) in muscle cells (White et al., 2014) and so-called heptad complex factors in hematopoietic stem cells (Solaimani Kartalaei et al., 2015), giving rise to a widespread cellular distribution (Hamann et al., 2015). Hobit comprises DNA-binding zinc finger domains, which closely resemble their homologous domains in Blimp-1 (van Gisbergen et al., 2012; Vieira Braga et al., 2015). In agreement with the presumed role of Hobit as transcription factor, multiple copies of the consensus binding sequence for Blimp-1/Hobit G(T/C)GAAAG(T/C)(G/T) (Doody et al., 2007) are identified in the 5'-region of *GPR56* (data not shown).

In mice, peripheral NK and T cells barely express GPR56 (www.immgen.org), which is in line

with the absence of Hobit in these cells (van Gisbergen et al., 2012). Interestingly, resting murine NK cells are minimally cytotoxic; they contain little granzyme B or perforin protein, whereas the respective mRNAs are abundant (Fehniger et al., 2007). Cytokine- and virus-induced activation of murine NK cells results in potent cytotoxicity, associated with a strong increase in granzyme B and perforin protein. It is tempting to speculate that murine NK and T cells do not express GPR56 due to the different ways they acquire cytotoxic capacity.

By studying two pairs of BFPP siblings with the recurrent R565W and C346S mutations in the second extracellular loop and the GAIN domain, respectively (Piao et al., 2004; 2005), which both obstruct cell surface expression of the receptor (Chiang et al., 2011; Jin et al., 2007), we found that GPR56 is not required for the development of functionally competent NK cells. Entirely GPR56-deficient NK cells with the R565W mutation killed K562 cells even more efficiently, indicated by enhanced degranulation, enhanced cytokine secretion, and enhanced induction of apoptosis in target cells. This observation provided a clue that GPR56 might regulate NK-cell cytotoxicity, a finding that we substantiated in NK-92 cells stably overexpressing GPR56. NK-92–GPR56 cells contained less granzyme B and TNF transcripts at resting state and produced less TNF and IFNγ protein upon PMA stimulation. Moreover, their ability to kill K562 was impaired, as indicated by reduced degranulation, reduced cytokine secretion, and reduced induction of apoptosis in target cells. Similar results were found in more killing-resistant THP1 and HeLa cells, altogether demonstrating that GPR56 inhibits NK-cell cytotoxicity.

Of note, no immune-related clinical phenotype has been reported for BFPP patients. This, however, is not surprising since effector functions of NK cells are balanced by activating and inhibitory signals that are simultaneously delivered to the cells following the engagement of several distinct families of transmembrane receptors (Caligiuri, 2008). GPR56 does not belong to a receptor family commonly associated with NK-cell regulation, such as immunoglobulin-like receptors and C-type lectins (Lanier, 2008; Pegram et al., 2011). GPR56 is a member of the aGPCR family. While the functional mechanism of aGPCRs is still poorly understood, evidence accumulates that they are true GPCRs that regulate wide cellular programs through the action of G proteins (Hamann et al., 2015; Monk et al., 2015). Indeed, the broad activity of GPR56 is indicated by its ability to control cytolytic proteins and pro-inflammatory cytokines, which present the two major arms of NK-cell activity. Moreover, we previously showed that GPR56 inhibits spontaneous and SDF-1-stimulated NK-cell migration (Peng et al., 2011). Studies in other cell types have implicated roles of GPR56 in generation and maintenance of the hematopoietic stem cell pool, cortical development, male fertility, muscle hypertrophy, and melanoma tumor growth and progression (Ackerman et al., 2015; Bae et al., 2014; Chen et al.,

2010; Giera et al., 2015; Piao et al., 2004; Saito et al., 2013; Solaimani Kartalaei et al., 2015; White et al., 2014; Xu et al., 2006).

Our data indicate that GPR56 executes its inhibitory activity in concert with the tetraspanin protein CD81. The GPR56–CD81 complex represents an early example of aGPCR in the tetraspanin web, an important membrane protein scaffold for regulating signal transmission (Little et al., 2004). More recently, the *Drosophila* aGPCR Flamingo was shown to interact in cis with the tetraspanin Van Gogh in the acquisition of planar cell polarity (Lawrence et al., 2008). The tetraspanin web is well known to modulate immune signaling, and CD81 has been shown to inhibit NK-cell functions when crosslinked (Crotta et al., 2002; Tseng and Klimpel, 2002). Our findings that the GPR56–CD81 complex on the NK-cell surface was quickly reduced and relocated to the contact points with the target cells suggested a role in regulating NK-cell activities. Indeed, ligation of GPR56 receptor by mAbs was found to dissociate the GPR56–CD81 complex, leading to enhanced NK-cell cytotoxicity and increased cytokine secretion. Based on these results, we suggest that GPR56 acts as a cell-autonomous NK-cell inhibitory receptor by laterally crosslinking with CD81. Removing GPR56 hence resulted in stronger NK-cell functions, as exemplified by the GPR56-deficient NK cells of BFPP patients as well as NK-92 and primary NK cells upon activation by PMA, cytokines, and contact with target cells.

At present, it is not known exactly how the GPR56–CD81 complex is recruited to the immune synapses upon NK–target cell conjugation. However, possible mechanisms can be envisioned based on earlier works. We have previously shown that while the majority of the GPR56 NTF–CTF heterodimeric receptor complex is located in the non-raft region, some of the GPR56 CTF is partitioned to the lipid raft microdomains (Chiang et al., 2011). Moreover, although lipid rafts and the tetraspanin-enriched microdomains (TEMs) are considered distinct membrane constitutions, co-clustering of lipid rafts and TEMs is possible upon cell activation or transformation (Krementsov et al., 2010; Ono, 2010).

Signaling molecules, including $G\alpha_{q/11}$, $G\alpha_{12/13}$, PKCα, RhoA, and mTOR, have been linked to GPR56 in different cell types (Ackerman et al., 2015; Giera et al., 2015; Iguchi et al., 2008; Little et al., 2004; Luo et al., 2011; Paavola et al., 2011; Stoveken et al., 2015; White et al., 2014). Of interest is the specific association with CD81 and $G\alpha_{q/11}$, reported by Little et al., in which CD81 was critical in promoting/stabilizing the GPR56–$G\alpha_{q/11}$ association (Little et al., 2004). The GPR56–CD81–$G\alpha_{q/11}$ complex was dynamically regulated: anti-CD81 mAb led to the uncoupling of $G\alpha_{q/11}$ from the GPR56–CD81 complex, while cell activation by PMA dissociated GPR56 from CD81 and $G\alpha_{q/11}$, leading to GPR56 internalization. In the present report, we applied a highly selective inhibitor of $G\alpha_{q/11/14}$, called FR900359 (Schrage et al., 2015). Of note, FR900359 did not restore cytotoxicity in NK-92–GPR56 cells. Thus, signaling capacity of the GPR56–CD81 complex in NK

cells does not rely on the engagement of $G\alpha_q$ proteins.

The ability to downregulate inhibitory receptors enables effector NK and T cells to unfold their full functional capacity. We found that PMA rapidly and completely downregulates GPR56 through PKC-mediated shedding and internalization. Moreover, an inflammatory milieu, created by the potent NK-cell activating cytokines IL-15 and IL-18 (Fehniger et al., 1999), caused PKC-dependent shedding of GPR56. Receptor shedding is a hallmark of aGPCRs and likely relates to the extended extracellular domains (Hamann et al., 2015). Previous studies indicate that in absence of the NTF, the CTF of GPR56 and other aGPCRs can overtly provide activating signals (Liebscher et al., 2014; Paavola and Hall, 2012; Paavola et al., 2011; 2014; Stephenson et al., 2013). GPR56 expression on cytotoxic lymphocytes will provide an interesting model to determine the fate and possible activities of an aGPCR upon activation-mediated release of its NTF and to explore therapeutic possibilities provided by the unique structure of this non-canonical GPCR.

EXPERIMENTAL PROCEDURES

Donors and cell isolation

PBMCs were isolated using a Lymphoprep gradient (Axis-Shield, Oslo, Norway) from fresh blood of healthy donors and four BFPP patients, diagnosed with single mutations in *GPR56*. Studied were two newly identified Dutch siblings of 46 and 49 years (1693C>T, R565W) and 2 previously described Palestinian siblings of 25 and 26 years (1036T>A, C346S) (Piao et al., 2004). Samples were obtained under informed consent and in accordance with ethical guidelines of the Academic Medical Center, Amsterdam, the Netherlands, the Radboudumc, Nijmegen, the Netherlands, and the Schneider Children's Medical Center, Petah Tiqva, Israel. $CD56^{+}CD3^{-}$ NK cells with ≥99% purity were isolated on a FACSAria™ III cell sorter (BD Biosciences, San Diego, CA, USA).

Stable transduction of cells

Generation of NK-92 cells stably overexpressing GPR56 has been described previously (Peng et al., 2011). The wild type and cleavage deficient mutant (T383A) of GPR56 were transduced using retroviruses in NK-92 cells. For gene knockdown, NK-92 cells were transduced using lentiviruses containing pKLO.1 plasmids with non-target scrambled short hairpin RNA (shRNA) (SHC002; sequence CCGGCAACAAGATGAAGAGCACCAACTC) from Sigma-Aldrich (St. Louis, MO, USA) or Eomes shRNA (TRCN0000013175; target sequence GCCCACTACAATGTGTTCGTA) and CD81 shRNA (TRCN0000057609; target sequence CCTGCTCTTCGTCTTCAATTT) from Open Biosystems (GE Healthcare, Lafayette, CO, USA). Cells were transduced in retronectin (Takara Bio Inc., Shiga, Japan)-coated plates and selected on 2 ng/ml puromycin (Sigma-Aldrich). NK-92 cells expressing pKLO.1 with Hobit shRNA (TRCN0000162720; CAGAAGAGCTTCACTCAACTT) or Jurkat cells expressing LZRS pBM-IRES-EGFP with Hobit fragment were generated previously (Vieira Braga et al., 2015). Transduced Jurkat cells were sorted to ≥95% purity on a FACSAria™ III cell sorter using green fluorescent protein (GFP) expression as selection marker.

Cytotoxicity assay

This assay employs 7-hydroxy-9H-(1,3-dichloro-9,9-dimethylacridin-2-one) (DDAO; Invitrogen, Carlsbad, CA, USA) to label target cells and 3,3'-dihexyloxacarbocyanine iodide (DiOC6; Invitrogen) to label live cells. Washed target cells (5×10^{6} cells/ml) were resuspended in 1 nM DDAO/phosphate-buffered saline (PBS), incubated at 37°C for 15 min in the dark, washed, and

resuspended in NK-92 medium. PBMCs or NK-92 stable cells were incubated at various effector/target ratios (5/1 to 1/5) with target cells at 37°C for 5 h, followed by addition of 0.1 µg/ml DiOC6 at 37°C for 15 min, and analysis by flow cytometry.

Cell stimulation

For activation of PKC, 1×10^6 cells/ml PBMCs were incubated for 2 h in medium plus 10 ng/ml PMA (Sigma-Aldrich). For cytokine stimulation, 1×10^6 cells/ml PBMCs were incubated for 12-24 h in medium containing 400 U/ml IL-2, 10 ng/ml IL-15, or 100 ng/ml IL-18 (all R&D Systems, Minneapolis, MN, USA), either alone or in combination, as indicated. For GPR56 Ab crosslinking, 48-well plates (Greiner bio-one, Frickenhausen, Germany) were coated with PBS containing mouse IgG, CG2, CG3, or CG5 at 37°C for 2 h followed by overnight coating at 4°C. After washing the plates with PBS, 2×10^6/ml NK-92–GPR56 cells or primary human NK cells were incubated in coated wells in complete NK-92 medium. Following 2 h of crosslinking at 37°C, 8×10^6/ml K562 cells were added to wells at E/T ratio=2. For cytokine production assay, supernatants were collected following 6 h of stimulation with K562 cells.

Pharmacological inhibitors were added for 1 h at 37°C prior to stimulation. Specific inhibitors of PKC (staurosporine, calphostin, bisindolylmaleimide I), PKB/Akt (Akt1/2 kinase inhibitor), PI3K (LY294002), MAP kinases ((Erk (U0126), JNK (SP600125) and p38 (SB 203580)), MMPs (GM6001), and dynamin (dynasore) were all obtained from Sigma-Aldrich. Inhibitors of ADAM10 and ADAM17 (GW) were a gift from GlaxoSmithkline, courtesy of Dr. A. Amour (Stevenage, United Kingdom); a second ADAM17 inhibitor (TNF484) was kindly provided by Dr. U. Neumann (Novartis, Basel, Switzerland). Gα signaling was inhibited using FR900359, a selective inhibitor of $G\alpha_{q/11/14}$ (Schrage et al., 2015).

Quantitative PCR

Total RNA was isolated with RNeasy mini kit (Qiagen, Hilden, Germany), and cDNA was synthesized using RevertAid First Strand cDNA Synthesis Kit (Thermo Fisher Scientific, Waltham, MA, USA). Relative gene expression levels were measured using Fast SYBR Green Master Mix (Applied Biosystems, Foster City, CA, USA) on a StepOnePlus™ System (Applied Biosystems) with the cycle threshold method. Primers are described in Extended Supplemental Procedures.

Flow cytometry

Staining of extracellular antigens was performed according to standard procedures. Abs are described in Extended Supplemental Procedures. For intracellular antigens, cells were first stained for surface molecules, followed by fixation with Foxp3 Transcription Factor Staining Buffer Set (eBioscience, San Diego, CA, USA) and incubation with antibodies directed against intracellular molecules. Flow cytometric analysis was performed on FACSCalibur, FACSCanto II, and LSRFortessa machines (BD Biosciences), and all data were analyzed with FlowJo software (Tree Star, Ashland, OR, USA).

For intracellular cytokine and degranulation staining, PBMCs and stable NK-92 cells were mixed with K562 in the presence of anti-CD107a and incubated at 37°C for 1 h in the dark. A mixture of brefeldin A (1 μg/ml; BD Biosciences) plus monensin (10 μg/ml; BD Biosciences) was then added, and samples were incubated for a further 5 h. Cells were labeled with antibodies recognizing extracellular antigens, fixed/permeabilized, stained for TNF and IFNγ, and examined by flow cytometry.

Enzyme-linked immunosorbent assay

TNF and IFNγ levels in culture supernatants were assessed using DuoSet ELISA Development Systems from R&D. Soluble GPR56 was quantified as described (Yang et al., 2015). Spectrophotometric analysis was performed at 450 nm wavelength on a SpectraMax M2 spectrophotometer (Molecular Devices, Sunnyvale, CA, USA) using Softmax Pro 5.3 software (Molecular Devices).

Indirect immunofluorescence

NK-92 were conjugated to K562 at 2/1 ratio, centrifuged at 25×g for 3 min at 4°C, and incubated for 30 min at 37°C. After conjugation, a total of 6×10^5 cells were gently resuspended and allowed to adhere to each poly-D-lysine coated coverslip (BD Biocoat) at 37°C for 30 min, centrifuged again at 30×g for 3 min, then washed by dipping in DPBS (Invitrogen) several times at room temperature. Subsequent fixation was carried out in 4% paraformaldehyde/PBS (Sigma-Aldrich) at room temperature for 20 min. Cells were blocked in PBS containing 2% normal goat serum and 0.5% BSA, and incubated first with mouse anti-CD81 mAb (TS81, Abcam, Cambridge, UK) and Alexa Fluor 594 conjugated goat anti-mouse IgG (Invitrogen), then washed and blocked again before staining with Alexa Fluor 488 conjugated mouse anti-GPR56 mAb (CG2). Permeabilization was carried out using 0.5% saponin (Sigma-Aldrich) and cells were stained subsequently with Alexa Fluor 647-conjugated anti-granzyme B mAb (GB11, BD Biosciences). Coverslips were mounted using ProLong Gold (with DAPI) mounting medium

(Invitrogen). Confocal images were captured on a Zeiss LSM 510 META confocal microscope (Carl Zeiss, Oberkochen, Germany) using a ×64 oil immersion objective. Single images were captured with an optical thickness of 1.5 μm. Analysis was performed using LSM510 META software (Carl Zeiss).

Immunoprecipitation

Cells were lysed in a 1% 3-[(3-cholamidopropyl)dimethylammonio]-1-propanesulfonate (CHAPS) buffer containing 20 mM Tris-HCl, pH7.4, 150 mM NaCl, 5 mM $MgCl_2$, 5% glycerol, and protease inhibitors including 1 mM sodium orthovanadate, 10 μg/ml aprotinin, 5 mM levamisole, 1 mM 4-(2-aminomethyl)benzenesulfonyl fluoride hydrochloride (AEBSF) and cOmplete™ protease inhibitor from Roche Diagnostics (Basel, Switzerland). Lysates were extracted on an end-over-end rotator at 4°C for 3 h and collected after removing insoluble fraction by centrifugation at 12,000 rpm for 25 min at 4°C. Supernatants were pre-cleared with Protein G Sepharose (Sigma-Aldrich) for at least 1 hour at 4°C on a rotator, or, for lysates collected from Ab-pre-treated cells, with mouse IgG conjugated to agarose (A0919; Sigma-Aldrich). Specific mAbs (4 μg) were then mixed with pre-cleared lysates (5×10^6 cell equivalents) and incubated on ice for 2 h before adding 20 μl of 1:1 diluted Protein G Sepharose beads. Immunoprecipitates were then collected overnight at 4°C on a rotator, washed five times with cold 1% CHAPS lysis buffer, eluted with 2× Laemmli buffer at 95°C for 8 min, and resolved on a 8% (for GPR56) or on a 12% (for CD81 and CD9) nonreduced SDS-PAGE. For re-IP, CD81 associated molecules were eluted with 1% Triton X-100 lysis buffer following anti-CD81 (clone TS81) IP. Eluates were then subjected for a second IP using anti-GPR56 (clone CG2) mAb. Immunoprecipitates were analyzed by immunoblotting using anti-GPR56 (clone CG4), anti-CD81 (clone 5A6), and anti-CD9 (clone MM2/57) mAbs.

Statistics

All results were analyzed by Excel (Microsoft, Redmond, WA, USA) or GraphPad Prism (GraphPad Software, La Jolla, CA, USA) and expressed as means ± standard error of the mean (SEM). A Student t test was used to determine P values. Significance was set at $P<0.05$.

SUPPLEMENTAL INFORMATION

Supplemental Information includes Supplemental experimental procedures and twelve figures and can be found with this article online at http://…

ACKNOWLEDGEMENTS

We thank the BFPP patients, their families, and the physicians Dr. D.J.J. Halley (Erasmus MC, Rotterdam), Dr. B. van Bon (Radboudumc, Nijmegen), and M. van Veldhoven (Cello, Rosmalen) for making this investigation possible. We thank Dr. X. Piao for helpful suggestions and B. Hooibrink and T.M. van Capel for help with cell sorting.

The study was supported by a scholarship from the Ministry of Education, Taiwan, and a fellowship from the European Federation of Immunological Societies (EFIS) to C.C.H. and by grants from the Ministry of Science and Technology, Taiwan (MOST101-2320-B-182-029-MY3 and MOST104-2320-B-182-035-MY3) and the Chang Gung Memorial Hospital (CMRPD1A0181-3, CMRPD1D0072-3, CMRPD1D0391-2) to H.H.L. as well as by the Thyssen Foundation (2015-00387) to K.P.J.M.v.G and J.H.. J.H. is a Mercator Fellow of the German Research Foundation (Research Unit 2149).

AUTHOR CONTRIBUTIONS

G.W.C., C.C.H., Y.M.P., F.A.V.B., N.A.M.K., and M.D.B.v.d.G. conducted the experiments, E.B.M.R., R.S., G.M.K., E.K., V.K., L.M., and R.A.W.v.L. provided advice and critical samples or reagents, G.W.C., C.C.H., K.P.J.M.v.G., H.H.L., and J.H designed the experiments and wrote the manuscript.

COMPETING FINANCIAL INTERESTS

The authors declare no competing financial interests.

REFERENCES

Ackerman, S.D., Garcia, C., Piao, X., Gutmann, D.H., and Monk, K.R. (2015). The adhesion GPCR Gpr56 regulates oligodendrocyte development via interactions with Gα12/13 and RhoA. Nat. Commun. *6*, 6122.

Araç, D., Boucard, A.A., Bolliger, M.F., Nguyen, J., Soltis, S.M., Südhof, T.C., and Brunger, A.T. (2012). A novel evolutionarily conserved domain of cell-adhesion GPCRs mediates autoproteolysis. Embo J. *31*, 1364–1378.

Baala, L., Briault, S., Etchevers, H.C., Laumonnier, F., Natiq, A., Amiel, J., Boddaert, N., Picard, C., Sbiti, A., Asermouh, A., et al. (2007). Homozygous silencing of T-box transcription factor EOMES leads to microcephaly with polymicrogyria and corpus callosum agenesis. Nat. Genet. *39*, 454–456.

Bae, B.-I., Tietjen, I., Atabay, K.D., Evrony, G.D., Johnson, M.B., Asare, E., Wang, P.P., Murayama, A.Y., Im, K., Lisgo, S.N., et al. (2014). Evolutionarily dynamic alternative splicing of GPR56 regulates regional cerebral cortical patterning. Science *343*, 764–768.

Björkström, N.K., Riese, P., Heuts, F., Andersson, S., Fauriat, C., Ivarsson, M.A., Björklund, A.T., Flodström-Tullberg, M., Michaëlsson, J., Rottenberg, M.E., et al. (2010). Expression patterns of NKG2A, KIR, and CD57 define a process of CD56dim NK-cell differentiation uncoupled from NK-cell education. Blood *116*, 3853–3864.

Caligiuri, M.A. (2008). Human natural killer cells. Blood *112*, 461–469.

Chen, G., Yang, L., Begum, S., and Xu, L. (2010). GPR56 is essential for testis development and male fertility in mice. Dev. Dyn. *239*, 3358–3367.

Chiang, N.-Y., Hsiao, C.-C., Huang, Y.-S., Chen, H.-Y., Hsieh, I.-J., Chang, G.-W., and Lin, H.-H. (2011). Disease-associated GPR56 mutations cause bilateral frontoparietal polymicrogyria via multiple mechanisms. J. Biol. Chem. *286*, 14215–14225.

Chiesa, Della, M., Falco, M., Parolini, S., Bellora, F., Petretto, A., Romeo, E., Balsamo, M., Gambarotti, M., Scordamaglia, F., Tabellini, G., et al. (2010). GPR56 as a novel marker identifying the CD56dull CD16+ NK cell subset both in blood stream and in inflamed peripheral tissues. Int. Immunol. *22*, 91–100.

Crotta, S., Stilla, A., Wack, A., D'Andrea, A., Nuti, S., D'Oro, U., Mosca, M., Filliponi, F., Brunetto, R.M., Bonino, F., et al. (2002). Inhibition of natural killer cells through engagement of CD81 by the major hepatitis C virus envelope protein. J. Exp. Med. *195*, 35–41.

Crotty, S., Johnston, R.J., and Schoenberger, S.P. (2010). Effectors and memories: Bcl-6 and Blimp-1 in T and B lymphocyte differentiation. Nat. Immunol. *11*, 114–120.

Daussy, C., Faure, F., Mayol, K., Viel, S., Gasteiger, G., Charrier, E., Bienvenu, J., Henry, T., Debien, E., Hasan, U.A., et al. (2014). T-bet and Eomes instruct the development of two distinct natural killer cell lineages in the liver and in the bone marrow. J. Exp. Med. *211*, 563–577.

Doody, G.M., Stephenson, S., McManamy, C., and Tooze, R.M. (2007). PRDM1/BLIMP-1 modulates IFN-gamma-dependent control of the MHC class I antigen-processing and peptide-loading pathway. J. Immunol. *179*, 7614–7623.

Elsen, G.E., Hodge, R.D., Bedogni, F., Daza, R.A.M., Nelson, B.R., Shiba, N., Reiner, S.L., and Hevner, R.F. (2013). The protomap is propagated to cortical plate neurons through an Eomes-dependent

intermediate map. Proc. Natl. Acad. Sci. USA *110*, 4081–4086.

Fauriat, C., Long, E.O., Ljunggren, H.-G., and Bryceson, Y.T. (2010). Regulation of human NK-cell cytokine and chemokine production by target cell recognition. Blood *115*, 2167–2176.

Fehniger, T.A., Shah, M.H., Turner, M.J., VanDeusen, J.B., Whitman, S.P., Cooper, M.A., Suzuki, K., Wechser, M., Goodsaid, F., and Caligiuri, M.A. (1999). Differential cytokine and chemokine gene expression by human NK cells following activation with IL-18 or IL-15 in combination with IL-12: implications for the innate immune response. J. Immunol. *162*, 4511–4520.

Fehniger, T.A., Cai, S.F., Cao, X., Bredemeyer, A.J., Presti, R.M., French, A.R., and Ley, T.J. (2007). Acquisition of murine NK cell cytotoxicity requires the translation of a pre-existing pool of granzyme B and perforin mRNAs. Immunity *26*, 798–811.

Freud, A.G., and Caligiuri, M.A. (2006). Human natural killer cell development. Immunol. Rev. *214*, 56–72.

Giera, S., Deng, Y., Luo, R., Ackerman, S.D., Mogha, A., Monk, K.R., Ying, Y., Jeong, S.-J., Makinodan, M., Bialas, A.R., et al. (2015). The adhesion G protein-coupled receptor GPR56 is a cell-autonomous regulator of oligodendrocyte development. Nat. Commun. *6*, 6121.

Hamann, J., Aust, G., Araç, D., Engel, F.B., Formstone, C., Fredriksson, R., Hall, R.A., Harty, B.L., Kirchhoff, C., Knapp, B., et al. (2015). International Union of Basic and Clinical Pharmacology. XCIV. Adhesion G Protein-Coupled Receptors. Pharmacol. Rev. *67*, 338–367.

Iguchi, T., Sakata, K., Yoshizaki, K., Tago, K., Mizuno, N., and Itoh, H. (2008). Orphan G protein-coupled receptor GPR56 regulates neural progenitor cell migration via a G alpha 12/13 and Rho pathway. J. Biol. Chem. *283*, 14469–14478.

Jin, Z., Tietjen, I., Bu, L., Liu-Yesucevitz, L., Gaur, S.K., Walsh, C.A., and Piao, X. (2007). Disease-associated mutations affect GPR56 protein trafficking and cell surface expression. Hum. Mol. Genet. *16*, 1972–1985.

Karpus, O.N., Veninga, H., Hoek, R.M., Flierman, D., van Buul, J.D., Vandenakker, C.C., vanBavel, E., Medof, M.E., van Lier, R.A.W., Reedquist, K.A., et al. (2013). Shear stress-dependent downregulation of the adhesion-G protein-coupled receptor CD97 on circulating leukocytes upon contact with its ligand CD55. J. Immunol. *190*, 3740–3748.

Kishore, A., Purcell, R.H., Nassiri-Toosi, Z., and Hall, R.A. (2016). Stalk-dependent and stalk-independent signaling by the adhesion G protein-coupled receptors GPR56 (ADGRG1) and BAI1 (ADGRB1). J. Biol. Chem. *291*, 3385-3394.

Knox, J.J., Cosma, G.L., Betts, M.R., and McLane, L.M. (2014). Characterization of T-bet and eomes in peripheral human immune cells. Front. Immunol. *5*, 217.

Krementsov, D.N., Rassam, P., Margeat, E., Roy, N.H., Schneider-Schaulies, J., Milhiet, P.-E., and Thali, M. (2010). HIV-1 assembly differentially alters dynamics and partitioning of tetraspanins and raft components. Traffic *11*, 1401–1414.

Langenhan, T., Aust, G., and Hamann, J. (2013). Sticky signaling--adhesion class G protein-coupled receptors take the stage. Sci. Signal. *6*, re3.

Lanier, L.L. (2008). Up on the tightrope: natural killer cell activation and inhibition. Nat. Immunol. *9*, 495–502.

Lawrence, P.A., Struhl, G., and Casal, J. (2008). Planar cell polarity: A bridge too far? Curr. Biol. *18*, R959–R961.

Lee, J., Zhang, T., Hwang, I., Kim, A., Nitschke, L., Kim, M., Scott, J.M., Kamimura, Y., Lanier, L.L., and Kim, S. (2015). Epigenetic modification and antibody-dependent expansion of memory-like NK cells in human cytomegalovirus-infected individuals. Immunity *42*, 431–442.

Liebscher, I., Schön, J., Petersen, S.C., Fischer, L., Auerbach, N., Demberg, L.M., Mogha, A., Cöster, M., Simon, K.-U., Rothemund, S., et al. (2014). A tethered agonist within the ectodomain activates the adhesion G protein-coupled receptors GPR126 and GPR133. Cell Rep. *9*, 2018–2026.

Lin, H.-H., Chang, G.-W., Davies, J.Q., Stacey, M., Harris, J., and Gordon, S. (2004). Autocatalytic cleavage of the EMR2 receptor occurs at a conserved G protein-coupled receptor proteolytic site motif. J. Biol. Chem. *279*, 31823–31832.

Little, K.D., Hemler, M.E., and Stipp, C.S. (2004). Dynamic regulation of a GPCR-tetraspanin-G protein complex on intact cells: central role of CD81 in facilitating GPR56-Galpha q/11 association. Mol. Biol. Cell *15*, 2375–2387.

Lopez-Vergès, S., Milush, J.M., Pandey, S., York, V.A., Arakawa-Hoyt, J., Pircher, H., Norris, P.J., Nixon, D.F., and Lanier, L.L. (2010). CD57 defines a functionally distinct population of mature NK cells in the human CD56dimCD16+ NK-cell subset. Blood *116*, 3865–3874.

Luo, R., Jeong, S.-J., Jin, Z., Strokes, N., Li, S., and Piao, X. (2011). G protein-coupled receptor 56 and collagen III, a receptor-ligand pair, regulates cortical development and lamination. Proc. Natl. Acad. Sci. USA *108*, 12925–12930.

Monk, K.R., Hamann, J., Langenhan, T., Nijmeijer, S., Schöneberg, T., and Liebscher, I. (2015). Adhesion G Protein-Coupled Receptors: From In Vitro Pharmacology to In Vivo Mechanisms. Mol. Pharmacol. *88*, 617–623.

Nagler, A., Lanier, L.L., Cwirla, S., and Phillips, J.H. (1989). Comparative studies of human FcRIII-positive and negative natural killer cells. J. Immunol. *143*, 3183–3191.

Ono, A. (2010). Relationships between plasma membrane microdomains and HIV-1 assembly. Biol. Cell *102*, 335–350.

Paavola, K.J., and Hall, R.A. (2012). Adhesion G protein-coupled receptors: signaling, pharmacology, and mechanisms of activation. Mol. Pharmacol. *82*, 777–783.

Paavola, K.J., Sidik, H., Zuchero, J.B., Eckart, M., and Talbot, W.S. (2014). Type IV collagen is an activating ligand for the adhesion G protein-coupled receptor GPR126. Sci. Signal. *7*, ra76.

Paavola, K.J., Stephenson, J.R., Ritter, S.L., Alter, S.P., and Hall, R.A. (2011). The N terminus of the adhesion G protein-coupled receptor GPR56 controls receptor signaling activity. J. Biol. Chem. *286*, 28914–28921.

Pegram, H.J., Andrews, D.M., Smyth, M.J., Darcy, P.K., and Kershaw, M.H. (2011). Activating and inhibitory receptors of natural killer cells. Immunol. Cell Biol. *89*, 216–224.

Peng, Y.-M., van de Garde, M.D.B., Cheng, K.-F., Baars, P.A., Remmerswaal, E.B.M., van Lier, R.A.W., Mackay, C.R., Lin, H.-H., and Hamann, J. (2011). Specific expression of GPR56 by human cytotoxic lymphocytes. J. Leukoc. Biol. *90*, 735–740.

Piao, X., Chang, B.S., Bodell, A., Woods, K., Benzeev, B., Topçu, M., Guerrini, R., Goldberg-Stern, H.,

Sztriha, L., Dobyns, W.B., et al. (2005). Genotype-phenotype analysis of human frontoparietal polymicrogyria syndromes. Ann. Neurol. *58*, 680–687.

Piao, X., Hill, R.S., Bodell, A., Chang, B.S., Basel-Vanagaite, L., Straussberg, R., Dobyns, W.B., Qasrawi, B., Winter, R.M., Innes, A.M., et al. (2004). G protein-coupled receptor-dependent development of human frontal cortex. Science *303*, 2033–2036.

Pierce, K.L., Premont, R.T., and Lefkowitz, R.J. (2002). Seven-transmembrane receptors. Nat. Rev. Mol. Cell Biol. *3*, 639–650.

Romee, R., Foley, B., Lenvik, T., Wang, Y., Zhang, B., Ankarlo, D., Luo, X., Cooley, S., Verneris, M., Walcheck, B., et al. (2013). NK cell CD16 surface expression and function is regulated by a disintegrin and metalloprotease-17 (ADAM17). Blood *121*, 3599–3608.

Saito, Y., Kaneda, K., Suekane, A., Ichihara, E., Nakahata, S., Yamakawa, N., Nagai, K., Mizuno, N., Kogawa, K., Miura, I., et al. (2013). Maintenance of the hematopoietic stem cell pool in bone marrow niches by EVI1-regulated GPR56. Leukemia *27*, 1637–1649.

Schlums, H., Cichocki, F., Tesi, B., Theorell, J., Beziat, V., Holmes, T.D., Han, H., Chiang, S.C.C., Foley, B., Mattsson, K., et al. (2015). Cytomegalovirus infection drives adaptive epigenetic diversification of NK cells with altered signaling and effector function. Immunity *42*, 443–456.

Schrage, R., Schmitz, A.-L., Gaffal, E., Annala, S., Kehraus, S., Wenzel, D., Büllesbach, K.M., Bald, T., Inoue, A., Shinjo, Y., et al. (2015). The experimental power of FR900359 to study Gq-regulated biological processes. Nat. Commun. *6*, 10156.

Solaimani Kartalaei, P., Yamada-Inagawa, T., Vink, C.S., de Pater, E., van der Linden, R., Marks-Bluth, J., van der Sloot, A., van den Hout, M., Yokomizo, T., van Schaick-Solernó, M.L., et al. (2015). Whole-transcriptome analysis of endothelial to hematopoietic stem cell transition reveals a requirement for Gpr56 in HSC generation. J. Exp. Med. *212*, 93–106.

Stephenson, J.R., Paavola, K.J., Schaefer, S.A., Kaur, B., Van Meir, E.G., and Hall, R.A. (2013). Brain-specific angiogenesis inhibitor-1 signaling, regulation, and enrichment in the postsynaptic density. J. Biol. Chem. *288*, 22248–22256.

Stoveken, H.M., Hajduczok, A.G., Xu, L., and Tall, G.G. (2015). Adhesion G protein-coupled receptors are activated by exposure of a cryptic tethered agonist. Proc. Natl. Acad. Sci. USA *112*, 6194–6199.

Tseng, C.-T.K., and Klimpel, G.R. (2002). Binding of the hepatitis C virus envelope protein E2 to CD81 inhibits natural killer cell functions. J. Exp. Med. *195*, 43–49.

van Gisbergen, K.P.J.M., Kragten, N.A.M., Hertoghs, K.M.L., Wensveen, F.M., Jonjic, S., Hamann, J., Nolte, M.A., and van Lier, R.A.W. (2012). Mouse Hobit is a homolog of the transcriptional repressor Blimp-1 that regulates NKT cell effector differentiation. Nat. Immunol. *13*, 864–871.

Vieira Braga, F.A., Hertoghs, K.M.L., Kragten, N.A.M., Doody, G.M., Barnes, N.A., Remmerswaal, E.B.M., Hsiao, C.-C., Moerland, P.D., Wouters, D., Derks, I.A.M., et al. (2015). Blimp-1 homolog Hobit identifies effector-type lymphocytes in humans. Eur. J. Immunol. *45*, 2945–2958.

Vivier, E., Tomasello, E., Baratin, M., Walzer, T., and Ugolini, S. (2008). Functions of natural killer cells. Nat. Immunol. *9*, 503–510.

Voehringer, D., Koschella, M., and Pircher, H. (2002). Lack of proliferative capacity of human effector and memory T cells expressing killer cell lectinlike receptor G1 (KLRG1). Blood *100*,

3698–3702.

Walzer, T., and Vivier, E. (2011). G-protein-coupled receptors in control of natural killer cell migration. Trends Immunol. *32*, 486–492.

White, J.P., Wrann, C.D., Rao, R.R., Nair, S.K., Jedrychowski, M.P., You, J.-S., Martínez-Redondo, V., Gygi, S.P., Ruas, J.L., Hornberger, T.A., et al. (2014). G protein-coupled receptor 56 regulates mechanical overload-induced muscle hypertrophy. Proc. Natl. Acad. Sci. USA *111*, 15756–15761.

Xu, L., Begum, S., Hearn, J.D., and Hynes, R.O. (2006). GPR56, an atypical G protein-coupled receptor, binds tissue transglutaminase, TG2, and inhibits melanoma tumor growth and metastasis. Proc. Natl. Acad. Sci. USA *103*, 9023–9028.

Yang, L., Chen, G., Mohanty, S., Scott, G., Fazal, F., Rahman, A., Begum, S., Hynes, R.O., and Xu, L. (2011). GPR56 Regulates VEGF production and angiogenesis during melanoma progression. Cancer Res. *71*, 5558–5568.

Yang, T.-Y., Chiang, N.-Y., Tseng, W.-Y., Pan, H.-L., Peng, Y.-M., Shen, J.-J., Wu, K.-A., Kuo, M.-L., Chang, G.-W., and Lin, H.-H. (2015). Expression and immunoaffinity purification of recombinant soluble human GPR56 protein for the analysis of GPR56 receptor shedding by ELISA. Protein Expr. Purif. *109*, 85–92.

Zhang, T., Scott, J.M., Hwang, I., and Kim, S. (2013). Cutting edge: antibody-dependent memory-like NK cells distinguished by FcRγ deficiency. J. Immunol. *190*, 1402–1406.

FIGURES

Figure 1. Hobit drives the expression of GPR56 in non-dividing, fully differentiated NK cells. (**A**) Expression of GPR56 on proliferating $CD56^{+}CD3^{-}$ NK cells was measured using CFSE dilution after 6 days of stimulation with 50 U/ml IL-2. Flow cytometry plots of one representative experiment (left) and quantification of the mean percentage of proliferating cells (right). (**B**) NK-92 cells were incubated with or without 50 U/ml IL-2 for 18 h and analyzed for cell cycle and expression of GPR56 by flow cytometry (left). Quantification of percentages of cells in G1, S, and G2/M phase, and relative geoMFI of GPR56 expression, compared to isotype controls (right). (**C**) Quantification of mRNA expression of surface molecules and transcription factors by RT-PCR in NK-92 cells, incubated with or without 50 U/ml IL-2 for 18 h. (**D**) Protein expression of surface molecules and transcription factors by $CD56^{+}CD3^{-}$ NK cells in cord blood and peripheral blood in relation to GPR56 expression, measured by flow cytometry. (**E**) Expression of GPR56 on long-lived memory-like NK cells, defined by absent/low expression of FcRγ and PLZF, determined by flow cytometry. (**F-H**) NK-92 cells overexpressing scrambled shRNA, Eomes shRNA, or Hobit shRNA were incubated with or without 50 U/ml IL-2 for 18 h and analyzed by flow cytometry for expression of Eomes, Hobit, and GPR56. Representative flow cytometry plots (F), quantification of Hobit and GPR56 protein expression, compared to isotype controls, by flow cytometry (G), and quantification of mRNA expression of GPR56 by RT-PCR (H). (**I-K**) Parental Jurkat cells and Jurkat cells overexpressing vector control or Flag-tagged Hobit were incubated with 10 μg/ml doxycycline for 48 h and analyzed by flow cytometry for expression of Flag and GPR56. Representative flow cytometry plots (I), quantification of Flag and GPR56 protein expression, compared to isotype controls, by flow cytometry (J), and quantification of mRNA expression of Hobit and GPR56 by RT-PCR (K). All data are means ± SEM of 3-5 independent experiments. *$p<0.05$, **$p<0.01$, ***$p<0.005$. See also Figure S1.

Figure 2. Normal development and functional competence of NK cells in BFPP patients. Shown are data of two Dutch siblings with the R565W mutation and age-matched healthy control donors. (**A**) Quantification of the percentage of NK cells among circulating lymphocytes and the expression of surface molecules, cytolytic proteins, and transcription factors by $CD56^{dim}CD3^{-}$ NK cells, measured by flow cytometry. (**B**) PBMCs were incubated with K562 target cells at an effector/target cell ratio of 1/1 for 5 h and analyzed by flow cytometry for K562 cell death, NK-cell degranulation (CD107a), and intracellular production of TNF and IFNγ. The control donor depicted here was analyzed in parallel with the Dutch patients. (**C**) Quantification of effector functions analyzed in (B), including additional control donors. All data

are means ± SEM. *p<0.05, **p<0.001, ****p<0.0001. See also Figure S2.

Figure 3. Inflammatory cytokines downregulate GPR56 in primary NK cells. PBMCs were stimulated as indicated and analyzed by flow cytometry. (**A**) Expression of GPR56 on $CD56^+CD3^-$ NK cells, stimulated for 6 h with the indicated amounts of PMA, alone or in combination with ionomycin. (**B**) Expression of GPR56 and CD16 on $CD56^+CD3^-$ NK cells, stimulated for 10 min or 2 h with 10 ng/ml PMA. (**C**) Expression of GPR56 on $CD56^+CD3^-$ NK cells pre-incubated for 1 h with 1 μM bisindolylmaleimide I (BIM), 100 μM dynasore (Dyn), 10 μM GM6001 (GM), or dynasore plus GM6001 before incubation with 10 ng/ml PMA for 2 h. (**D**) Expression of GPR56 and CD16 on $CD56^+CD3^-$ NK cells, pre-stained with anti-GPR56 or anti-CD16 mAb prior to incubation with 10 ng/ml PMA for 2 h. (**E**) Culture supernatants of PBMCs, pre-incubated for 1 h with inhibitors before incubation with 10 ng/ml PMA for 2 h, were analyzed by ELISA for soluble GPR56. (**F**) Expression of GPR56 and CD16 on $CD56^+CD3^-$ NK cells stimulated for 12 or 24 h with 500 U/ml IL-2, 10 ng/ml IL-15, 100 ng/ml IL-18, or IL-15 plus IL-18. Representative flow cytometry plots (left) and quantification of relative geoMFI (right). (**G**) Expression of GPR56 and CD16 on $CD56^+CD3^-$ NK cells pre-incubated with inhibitors and then stimulated for 12 or 24 h with IL-15 plus IL-18. (**H**) Quantification of mRNA expression of Hobit and GPR56 by RT-PCR in PBMCs, incubated with 10 ng/ml PMA for 2 h or with 10 ng/ml IL-15 plus 100 ng/ml IL-18 for 12 and 24 h. All data are means ± SEM of 4 independent experiments. *p<0.05, **p<0.01, ***p<0.005. See also Figure S3.

Figure 4. GPR56 expression in NK-92 cells reduces cytotoxic capacity. Vector-transduced (Neo) and GPR56-overexpressing NK-92 cells were studied. (**A**,**B**) Quantification of mRNA and protein expression of the cytolytic proteins perforin and granzyme B by RT-PCR (A) and flow cytometry (B) in NK-92–Neo and NK-92–GPR56 cells. (**C**,**D**) Quantification of mRNA and protein expression of the cytokines TNF and IFNγ by RT-PCR (C) and flow cytometry (D) in NK-92–Neo and NK-92–GPR56 cells. Protein expression was determined after stimulating cells with 10 nM PMA for 3 and 6 h. (**E**) Secretion of TNF and IFNγ by NK-92–Neo and NK-92–GPR56 cells treated with PMA for 1, 3, and 6 h, measured by ELISA. (**F**,**G**) NK-92 cells were incubated with fluorescently labeled or unlabeled K562 target cell (E/T=effector/target cell ratio) for 5 h and analyzed by flow cytometry for K562 cell death, NK-cell degranulation (CD107a), and intracellular production of TNF and IFNγ. Shown are representative flow cytometry plots (F) and quantification (G). (**H**) Secretion of TNF and IFNγ by NK-92–Neo and NK-92–GPR56 cells cultured with K562 target cells for 1, 3, and 6 h, measured by ELISA. All data are means ± SEM of 3 independent experiments. ***p<0.005. See also Figure S4.

Figure 5. GPR56-CD81 complexes at the immune synapse repress cytotoxicity and cytokine production of NK cells. (**A**) Surface CD81 and GPR56, and intracellular granzyme B of NK-92–K562 cell conjugates were sequentially stained and detected using confocal microscopy. DAPI staining defined the morphology of nuclei. Scale bars, 10 μm. (**B**) 1% CHAPS cell lysate was immunoprecipitated with either anti-GPR56 or anti-CD81 mAb, as indicated. The presence of GPR56, CD81, and CD9 was revealed by immunoblotting (IB) using specific mAbs. (**C**) NK-92–GPR56 cells were incubated in the absence (untreated) or presence of 10 μg/ml of GPR56 mAbs at 37°C or 0°C for 15 min before lysate collection for IP using anti-GPR56 mAb. Mouse IgG_1 was used as an isotype control. The presence of CD81 in each immunoprecipitate was revealed by immunoblotting. (**D-G**) NK-92–GPR56 (D,E) or human primary NK cells (F,G) were incubated in plates pre-coated with or without various anti-GPR56 mAbs (10 μg/ml) as indicated for 2 h before adding K562 target cells. Percentage of dead target cells in each sample was quantified by flow cytometric analysis following 4 h of co-culture (D,F), and amount of TNF and IFNγ released into medium during 6 h incubation was measured by ELISA (E,G). Data are representative of 3 independent experiments; values indicate the mean ± SEM. ***$p<0.005$. See also Figure S5, Figure S6, and Figure S7.

Figure 1

Fig.1

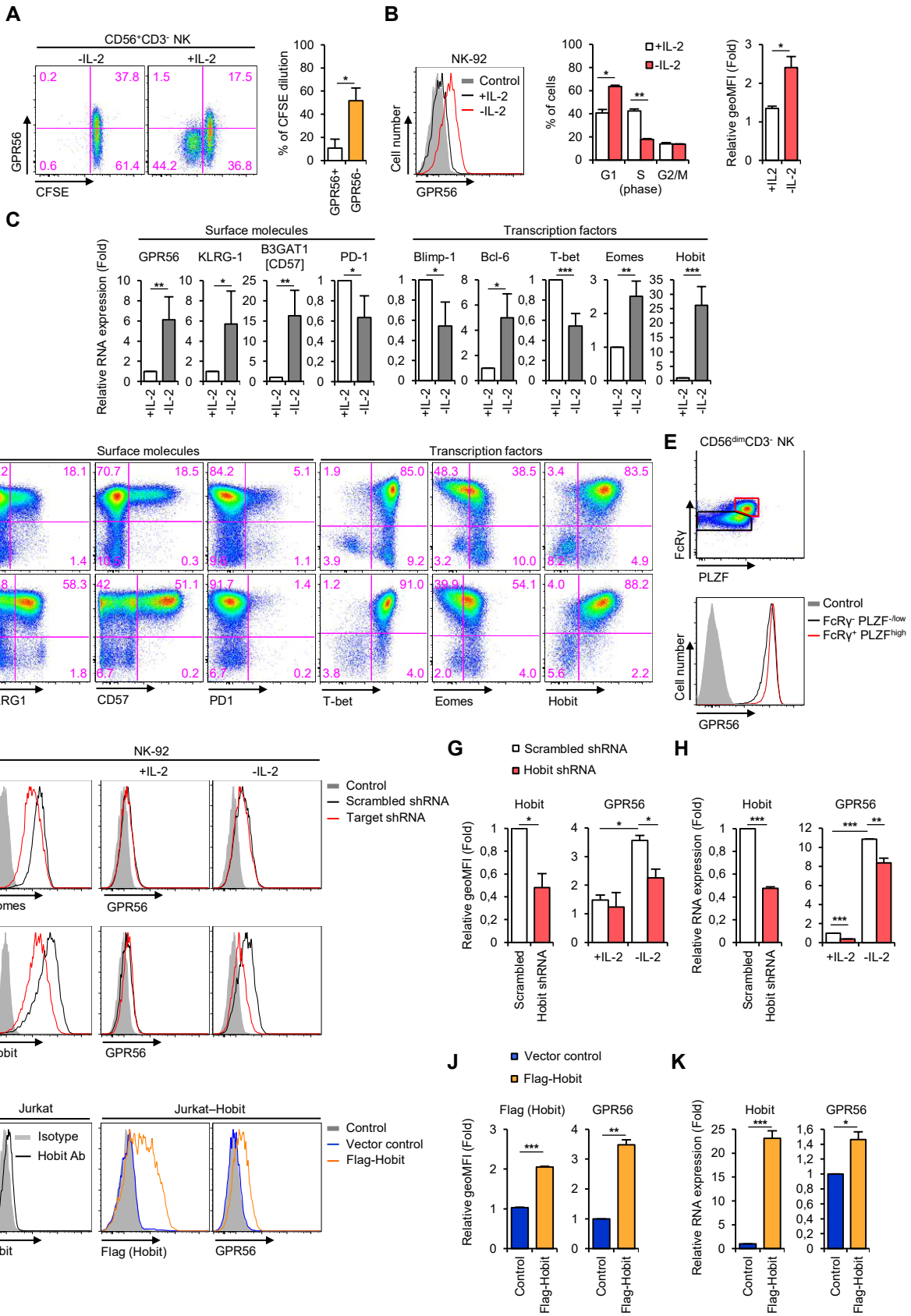

Figure 2

Fig.2

A

Cells/Molecule	Controls (n=5)	R565W-BFPP (n=2)	*p* value
CD56⁺CD3⁻ NK	13.5 ± 7.9	7.8 ± 1.0	0.4283
GPR56#	5610.7 ± 560.8	133 ± 0.0	****< 0.0001
CD16#	4079.3 ± 819.1	4499.0 ± 840.0	0.6087
CD27	7.5 ± 3.4	10.0 ± 2.4	0.4648
CD94#	837.4 ± 171.2	458.5 ± 6.5	*0.0113
KLRG1	61.6 ± 9.6	52.3 ± 5.1	0.3215
CD57	49.4 ± 7.0	43.4 ± 10.7	0.4861
PD1	3.2 ± 1.6	1.5 ± 0.0	0.2526
CD81#	2765 ± 846.1	2142.5 ± 111.5	0.3810
DNAM1	96.6 ± 2.6	89.5 ± 0.3	0.5261
NKp30	96.7 ± 3.0	92.3 ± 1.3	0.3587
NKp44	32.5 ± 2.1	32.3 ± 1.0	0.5438
NKp46	78.8 ± 10.6	85.9 ± 2.7	0.1383
NKG2a	8.7 ± 3.8	7.3 ± 0.0	0.5679
NKG2c	29.8 ± 1.7	24.8 ± 0.6	0.2200
NKG2d	99.7 ± 0.1	93.9 ± 1.4	0.0655
KIR2DL1/S1	26.8 ± 6.2	3.5 ± 3.4	**0.0053
KIR2DL2/L3	30.6 ± 4.6	35.8 ± 0.9	0.0788
KIR3DL1	25.8 ± 10.9	26.5 ± 1.1	0.5826
Perforin#	8285 ± 1600.5	4304 ± 503	0.0951
Granzyme B#	2758 ± 991.2	2017.5 ± 19.5	0.2863
T-bet	85.3 ± 10.2	69.1 ± 0.8	0.1166
Eomes	43.4 ± 21.9	66.1 ± 10.3	0.2890
Hobit	73.0 ± 12.8	84.9 ± 2.4	0.3190

% positive cells or #geoMFI ± SEM in CD56^{dim}CD3^{-}NK

B

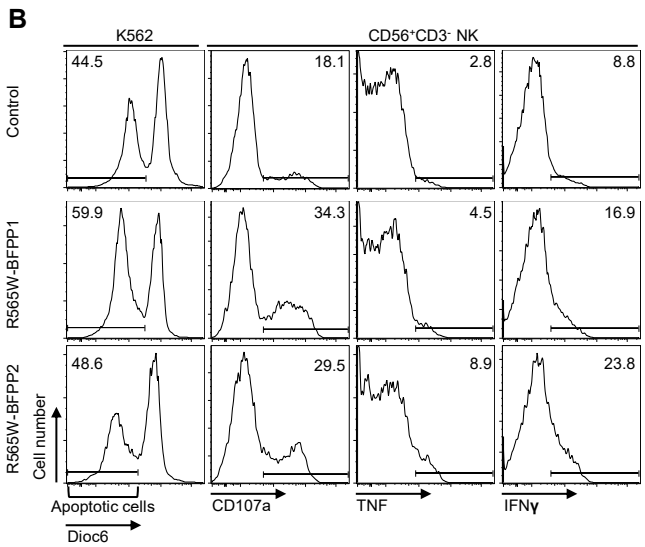

C

Effector function	Controls (n=6)	R565W-BFPP (n=2)	*p* value
Apoptotic K562 cells	30.2 ± 8.9	54.3 ± 5.65	*0.0414
CD107a	17.3 ± 5.2	31.9 ± 2.4	**0.0072
TNF	3.2 ± 1.2	6.7 ± 2.2	*0.0354
IFNγ	14.1 ± 4.3	20.4 ± 3.45	0.0904

% of positive cells ± SEM

Figure 3

Fig.3

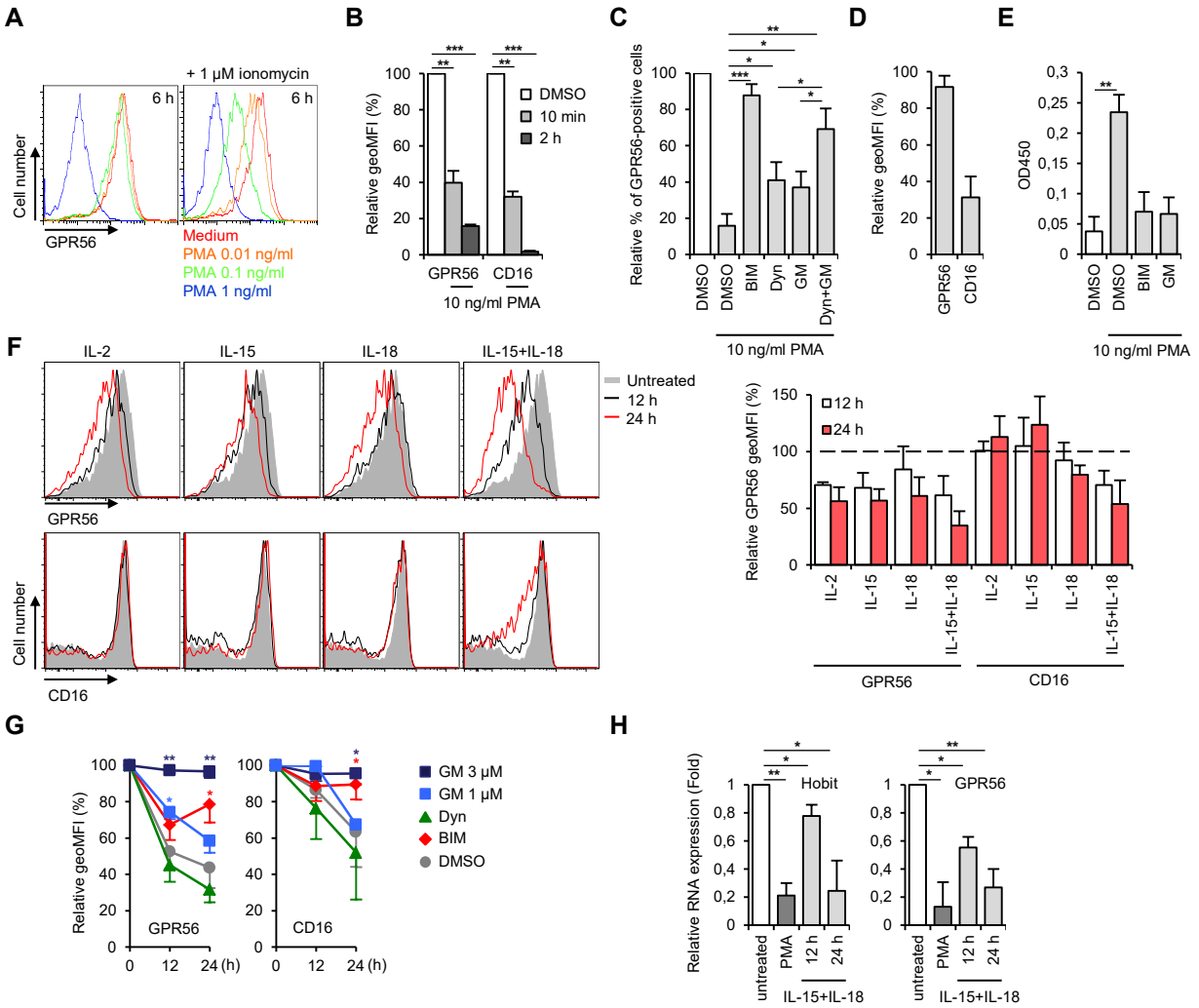

Figure 4

Fig.4

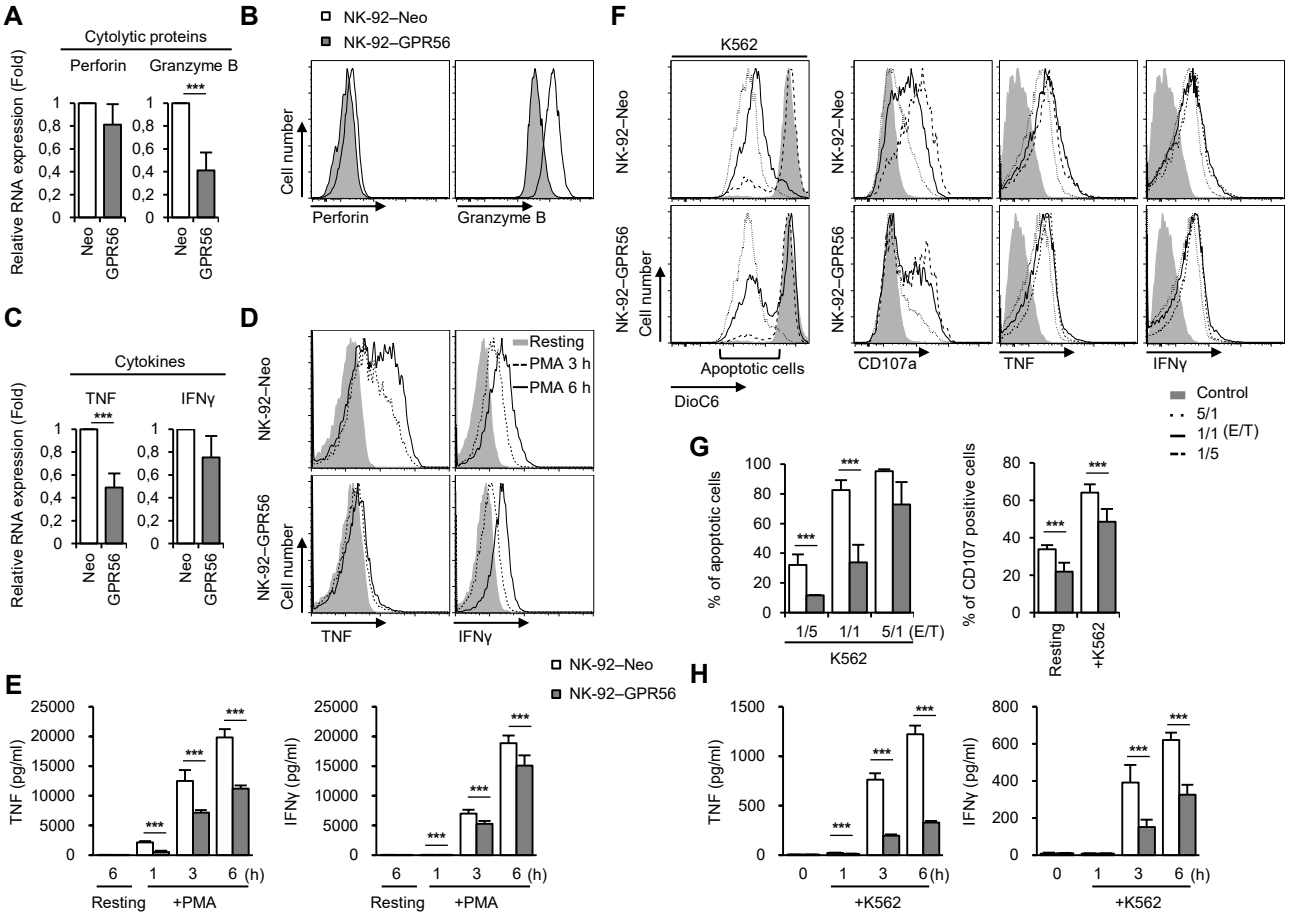

Figure 5

Fig.5

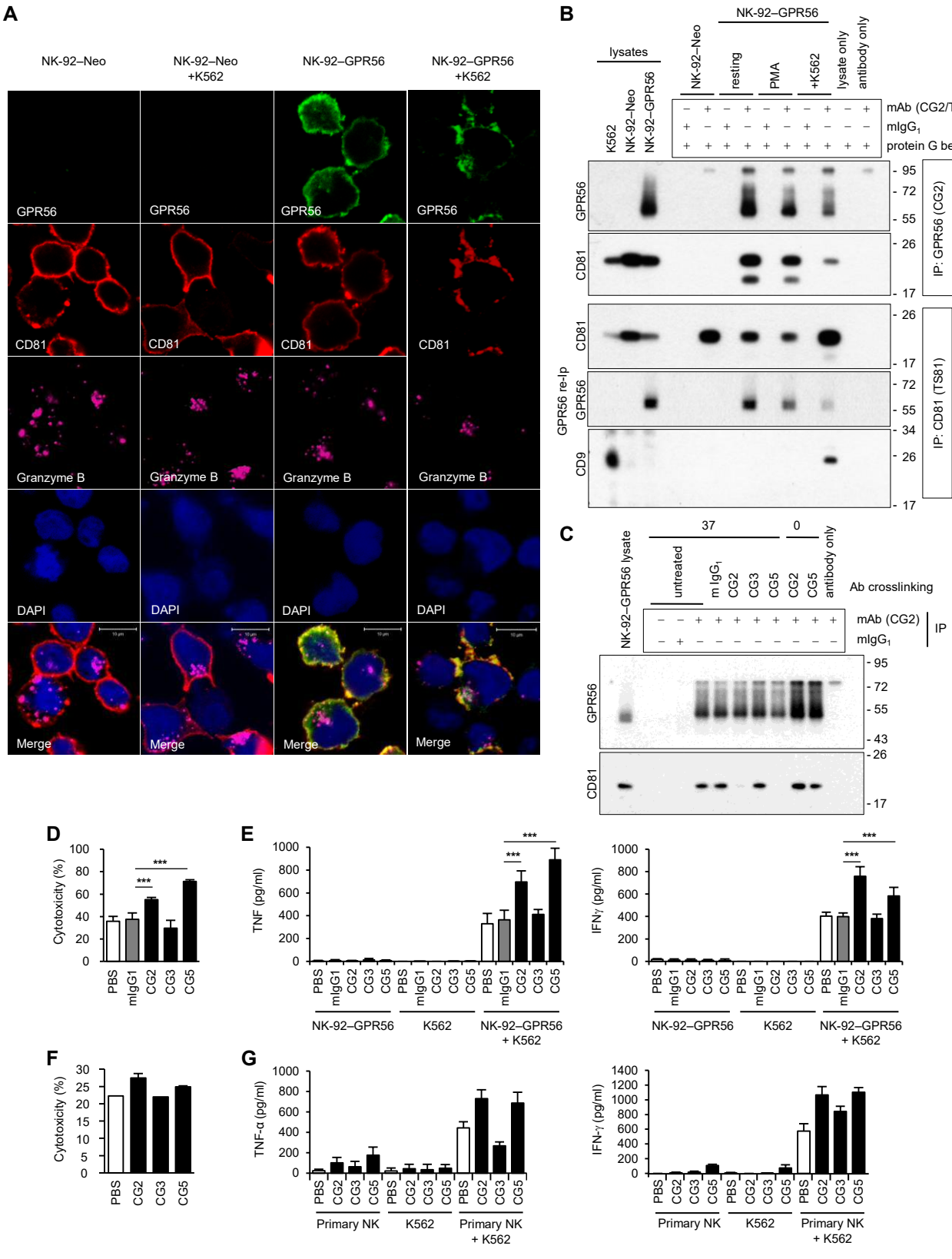

SUPPLEMENTAL INFORMATION

The adhesion G protein-coupled receptor GPR56/ADGRG1 is an inhibitory receptor on human NK cells

Gin-Wen Chang[1,10], Cheng-Chih Hsiao[2,10], Yen-Ming Peng[1], Felipe A. Vieira Braga[3], Natasja A.M. Kragten[3], Ester B. M. Remmerswaal[2,4], Martijn D. B. van de Garde[2], Rachel Straussberg[5], Gabriele M. König[6], Evi Kostenis[6], Vera Knäuper[7], Linde Meyaard[8], René A.W. van Lier[3], Klaas P.J.M. van Gisbergen[3], Hsi-Hsien Lin[1,9,11,*], and Jörg Hamann[2,11,*]

[1]Graduate Institute of Biomedical Sciences, College of Medicine, Chang Gung University, 333 Tao-Yuan, Taiwan; [2]Department of Experimental Immunology and [4]Renal Transplant Unit, Academic Medical Center, University of Amsterdam, 1105 AZ Amsterdam, The Netherlands; [3]Department of Hematopoiesis, Sanquin Research and Landsteiner Laboratory, Academic Medical Center, University of Amsterdam, 1066 CX Amsterdam, The Netherlands; [5]Department of Child Neurology, Neurogenetics Clinic, Schneider Children's Medical Center, Petach Tikva and Sackler Faculty of Medicine, Tel Aviv University, Tel Aviv 69978, Israel; [6]Institute for Pharmaceutical Biology, University of Bonn, 53115 Bonn, Germany; [7]Dental School, Cardiff University, Cardiff CF14 4XN, United Kingdom; [8]Department of Immunology, University Medical Center Utrecht, 3584 EA Utrecht, The Netherlands; [9]Chang Gung Immunology Consortium and Department of Anatomic Pathology, Chang Gung Memorial Hospital-Linkou, 333 Tao-Yuan, Taiwan. [10]Co-first author, [11]Co-senior author

Supplemental information: 5 pages, 5 supplemental references, and 7 supplemental figures

***Correspondence:** Dr. Jörg Hamann, Department of Experimental Immunology, K0-144, Academic Medical Center, University of Amsterdam, Meibergdreef 9, 1105 AZ Amsterdam, The Netherlands. E-mail: j.hamann@amc.uva.nl and Dr. Hsi-Hsien Lin, Department of Microbiology and Immunology, College of Medicine, Chang Gung University, 259 Wen-Hwa 1st Road, Kwei-Shan, 333 Tao-Yuan, Taiwan. E-mail: hhlin@mail.cgu.edu.tw

SUPPLEMENTAL EXPERIMENTAL PROCEDURES

Cell culture

Cells were maintained in the following media supplemented with 10% heat-inactivated fetal bovine serum (FBS): Peripheral blood mononuclear cells (PBMCs), purified $CD56^+CD3^-$ NK cells, and monocytic THP-1 cells in Roswell Park Memorial Institute (RPMI) 1640 medium; erythroleukemic K562 cells and Jurkat T cells in Iscove's modified Dulbecco's medium (IMDM); HeLa cells in Dulbecco's Modified Eagle Medium (DMEM). Human NK-92 cells were cultured in nucleoside-free α-Minimum Essential Medium (α-MEM) containing 12.5 % FBS, 12.5% horse serum, 0.2 mM inositol, 0.1 mM 2-mercaptoethanol, 0.02 mM folic acid, and 100 IU/ml IL-2. Cell culture media and supplements were obtained from Invitrogen (Carlsbad, CA, USA).

Cytotoxicity assay

Alternative to the method described in the main text, target cells were labeled with carboxyfluorescein succinimidyl ester (CFSE; Invitrogen) and dead cells with 7-aminoactinomycin D (7-AAD; Invitrogen). Washed target cells (5×10^6 cells/ml) were resuspended in phosphate-buffered saline (PBS) containing CFSE (2 μM for K562, 1 μM for THP-1, and 2.5 μM for HeLa) and incubated at 37°C for 10 min in the dark, followed by quenching the CFSE staining for 5 min on ice. Washed cells were resuspended in NK92 medium. NK-92 stable cells were incubated at various effector/target ratios (40/1 to 1/10) with target cells at 37°C for 4 h, followed by addition 0.5 ml of ice-cold Dulbecco's PBS (DPBS; Invitrogen), containing 1% bovine serum albumin (BSA) and 5 μg/ml 7-AAD, for 15 min in the dark, and analysis by flow cytometry.

Cell stimulation

Next to the conditions described in the main text, CD16 was crosslinked by pre-coating flat 96-well microplates (Corning, Corning, NY, USA) with 10 μg/ml goat anti-mouse immunoglobulin (Ig)G in PBS at 37°C for 2 h. Plates were washed twice with PBS and coated with 10 μg/ml purified anti-CD16 in PBS at 4°C for overnight. Then, plates were washed twice with PBS and blocked with RPMI 1640 medium/10% FBS at 37°C for 1 h. 2×10^6 cells/ml purified $CD56^+CD3^-$ NK cells were added to the plates.

Proliferation assay

PBMCs were washing three times in PBS, resuspended at 5×10^6 cells/ml in PBS, and labeled with 2.5 μM CFSE by shaking at 37°C for 10 min. Cells were washed three times and subsequently cultured in RPMI 1640 medium with or without 50 U/ml IL-2 for 5 days.

Conjugation assay

Target cells were labeled with CFSE as described above. 1×10^6 of labeled target cells were mixed with 5×10^5 NK-92 cells at an effector/target ratio of 1/2. The cell mixture was centrifuged at 25×g for 3 min at 4°C, then placed in a 37°C water bath for the desired lengths of time. After conjugation, cells were gently resuspended, fixed in 2% ice-cold paraformaldehyde/ PBS for 30 min, then subjected to Ab staining using either allophycocyanin (APC)-conjugated anti-CD56 mAb (if K562 and HeLa were used as targets) or APC-conjugated anti-CD2 mAb (if THP-1 was used as a target). Conjugation was analyzed by flow cytometry (FL-1 *versus* FL-4), and measured by percentage of NK cells that formed conjugates with target cells as calculated by the ratio of two-color events to total effector cell events.

Quantitative PCR

The following primers were used: *ADGRG1* (forward 5'-GATTGCTGGCCTGTTGTAG-3', reverse 5'-GAATGATGGCTCCCTGTCC-3'); *B3GAT1* (forward 5'-GAAGCCAGGCCTACTTCAAGCT-3', reverse 5'-GTTGAGGGTGACAAGTTCTCGAA-3'); *BCL6* (forward 5'-AACCTGAAAACCCACACTCG-3', reverse 5'-CTGGCTTTTGTGACGGAAAT-3'); *CD81* (forward 5'-AGGGCTGCACCAAGTGC-3', reverse 5'-TGTCTCCCAGCTCCAGATA-3'); *GZMB* (forward 5'-TGGGGGACCCAGAGATTAAAA-3', reverse 5'-TTTCGTCCATAGGAGACAATGC-3'); *KLRG1* (forward 5'-AACGGACAATCAGGAAATGAG-3', reverse 5'-CCTTGAGAAGTTTAGAGGTGATCC-3'); *PDCD1* (forward 5'-CTCAGGGTGACAGAGAGAAG-3', reverse 5'-GACACCAACCACCAGGGTTT-3'); *PRDM1* (forward 5'-GTGTCAGAACGGGATGAACA-3', reverse 5'-GCTCGGTTGCTTTAGACTGC-3'); *PRF1* (forward 5'-CGCCTACCTCAGGCTTATCTC-3', reverse 5'-CCTCGACAGTCAGGCAGTC-3'); *TBR1* (forward 5'-ACTGGTTCCCACTGGATGAG-3', reverse 5'-CCACGCCATCCTCTGTAACT-3'); *TBX1* (forward 5'-GGGAAACTAAAGCTCACAAAC-3', reverse 5'-CCCCAAGGAATTGACAGTTG-3'); *TNF* (forward 5'-CCCAGGGACCTCTCTCTAATCA-3', reverse 5'-AGCTGCCCCTCAGCTTGAG-3'); *ZNF683* (forward 5'-CATATGTGGCAAGAGCTTTGG-3', reverse 5'-GGCAAGTTGAGTGAAGCTCT-3'). Expression of specific genes was normalized to human *GAPDH* (forward 5'-GAAGGTGAAGGTCGGAGTC-3', reverse 5'-GAAGATGGT GATGGGATTTC-3') as endogenous control.

Antibodies and flow cytometry

Conjugated mAbs with the following specificity were used: anti-GPR56 (clone CG4; Biolegend, San Diego, CA, USA); anti-CD2 (clone RPA-2.10; BD Biosciences, San Diego, CA, USA); anti-CD3 (clone SK7 and UCHT1; BD Biosciences); anti-CD9 (clone ML13; BD Biosciences); anti-CD16 (clone 3G8; BD Biosciences); anti-CD56 (clone NAM16.2; BD Biosciences); anti-CD57 (clone NK-1; BD Biosciences); anti-CD81 (clone 1D6-CD81; eBioscience, San Diego, CA, USA); anti-CD94 (clone HP-3D9; BD Biosciences); anti-CD107a (clone H4A3; eBioscience); anti-CD158a/h (KIR2DL1/S1; clone EB6B; Beckman Coulter, Miami, FL, USA); anti-CD158b (KIR2DL2/L3; clone GL183; Beckman Coulter); anti-CD158e (KIR3DL1; clone DX9; BD Biosciences); anti-CD159a (NKG2a; clone #131411; R&D Systems); anti-CD159c (NKG2c; clone #134591; R&D Systems); anti-CD226 (DNAM-1; clone 11A8; Biolegend); anti-CD279 (PD-1; clone EH12.1; BD Biosciences); anti-CD314 (NKG2d; clone 1D11; Biolegend); anti-CD335 (NKp46; clone 9E2; AbD Serotec, Kidlington, UK); anti-CD336 (NKp44; clone P44-8; Biolegend); anti-CD337 (NKp30; clone P30-15; Biolegend); anti-KLRG1 (kindly provided by Prof. H.P. Pircher, Freiburg) (Marcolino et al., 2004); anti-FcRγ (rabbit polyclonal antibody; Millipore, Bedford, MA, USA); anti-perforin (clone δG9; BD Biosciences); anti-granzyme B (clone GB11; BD Biosciences); anti-TNF (clone MAb11; eBioscience); anti-IFNγ (clone 4s.B3; eBioscience); anti-T-bet (clone 4B10; Biolegend); anti-Eomes (clone WD1928; eBioscience); anti-PLZF (clone R17-809; BD Biosciences); anti-mouse IgM (clone II/41; eBioscience).

The following purified mAb were used: anti-GPR56 (clone CG2, CG4, CG3, and CG5; Biolegend and (Peng et al., 2011)); anti-CD9 (clone MM2/57; Millipore, Bedford, MA, USA); anti-CD16 (clone 3G8; Biolegend); anti-CD81 (clone TS81 and 5A6; Abcam, Cambridge, UK and Santa Cruz Biotechnology, Dallas, TX, USA); anti-Hobit (Vieira Braga et al., 2015); mouse IgG1 (clone MOPC-21, BD Biosciences).

Collagen I and III (Abcam) was conjugated with fluorescein-5-Isothiocyanate (FITC, Invitrogen) and used to explore ligand binding (Van de Walle et al., 2005).

To analyze cell cycle phase distribution, NK-92 cells were washed with cold PBS and fixed in 70% ethanol for 1 h. Fixed cells were stained with 20 µg/ml propidium iodide/0.1% Triton-X (both from Sigma-Aldrich, St. Louis, MO, USA) in the presence of 200 µg/ml RNaseA (Qiagen, Hilden, Germany) for 30 min at room temperature in the dark and analyzed by flow cytometry.

SUPPLEMENTAL REFERENCES

Lebbink, R.J., de Ruiter, T., Adelmeijer, J., Brenkman, A.B., van Helvoort, J.M., Koch, M., Farndale, R.W., Lisman, T., Sonnenberg, A., Lenting, P.J., et al. (2006). Collagens are functional, high affinity ligands for the inhibitory immune receptor LAIR-1. J. Exp. Med. *203*, 1419–1425.

Marcolino, I., Przybylski, G.K., Koschella, M., Schmidt, C.A., Voehringer, D., Schlesier, M., and Pircher, H. (2004). Frequent expression of the natural killer cell receptor KLRG1 in human cord blood T cells: correlation with replicative history. Eur. J. Immunol. *34*, 2672–2680.

Peng, Y.-M., van de Garde, M.D.B., Cheng, K.-F., Baars, P.A., Remmerswaal, E.B.M., van Lier, R.A.W., Mackay, C.R., Lin, H.-H., and Hamann, J. (2011). Specific expression of GPR56 by human cytotoxic lymphocytes. J. Leukoc. Biol. *90*, 735–740.

Van de Walle, G.R., Vanhoorelbeke, K., Majer, Z., Illyés, E., Baert, J., Pareyn, I., and Deckmyn, H. (2005). Two functional active conformations of the integrin {alpha}2{beta}1, depending on activation condition and cell type. J. Biol. Chem. *280*, 36873–36882.

Vieira Braga, F.A., Hertoghs, K.M.L., Kragten, N.A.M., Doody, G.M., Barnes, N.A., Remmerswaal, E.B.M., Hsiao, C.-C., Moerland, P.D., Wouters, D., Derks, I.A.M., et al. (2015). Blimp-1 homolog Hobit identifies effector-type lymphocytes in humans. Eur. J. Immunol. *45*, 2945–2958.

SUPPLEMENTAL FIGURES

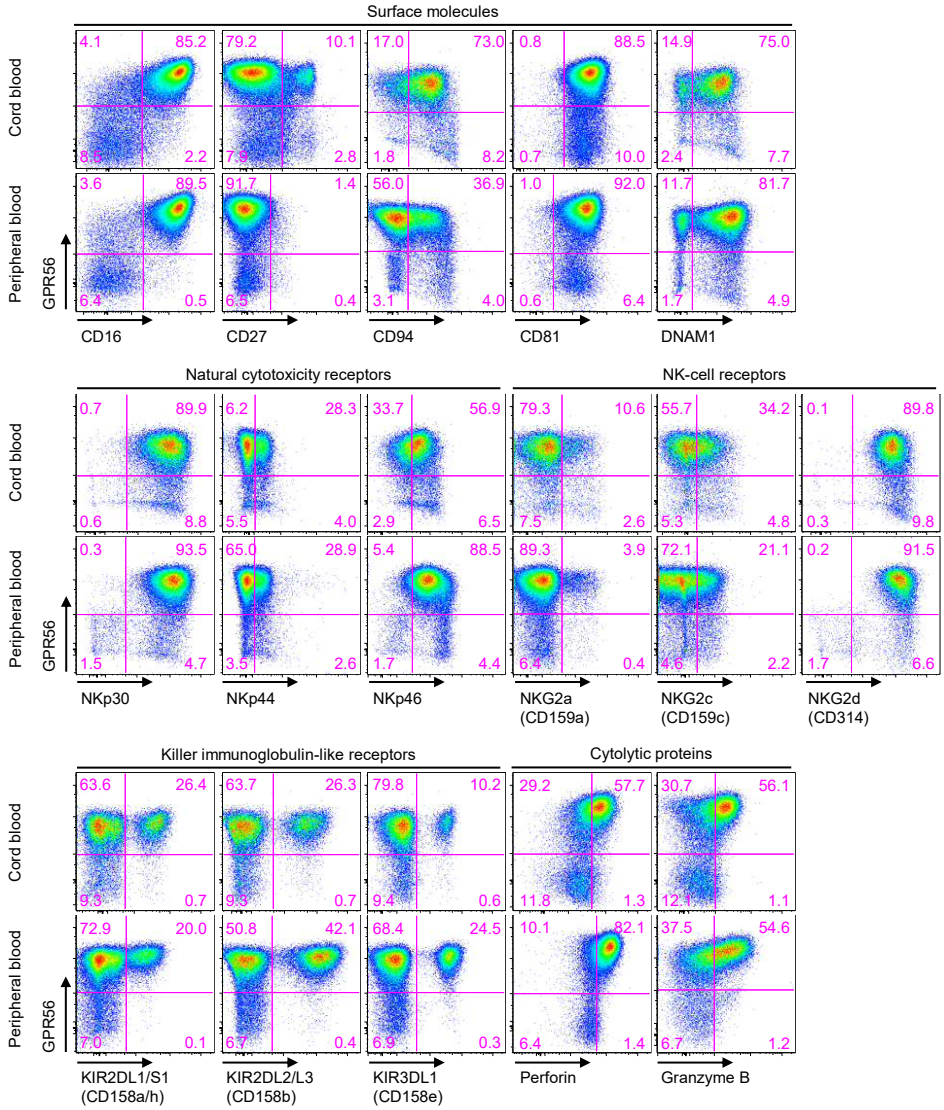

Figure S1. Expression profiling of NK cells from cord blood and peripheral blood in relation to GPR56 expression. Related to Figure 1. Flow-cytometric analysis of $CD56^{+}CD3^{-}$ NK cells for expression of various surface molecules, natural cytotoxicity receptors, NK-cell receptors, killer immunoglobulin-like receptors, and cytolytic proteins, measured by flow cytometry.

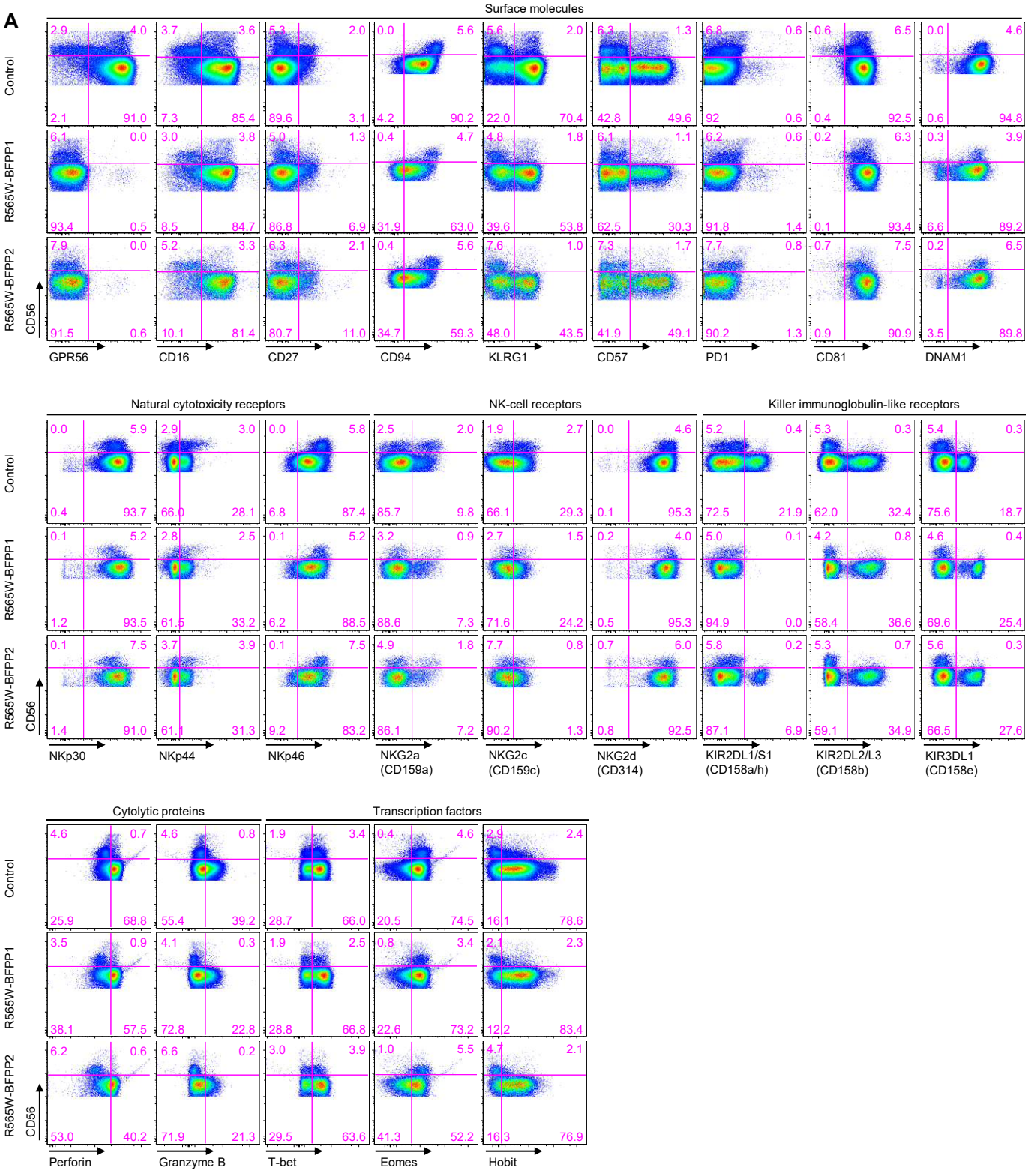

Continued on next page

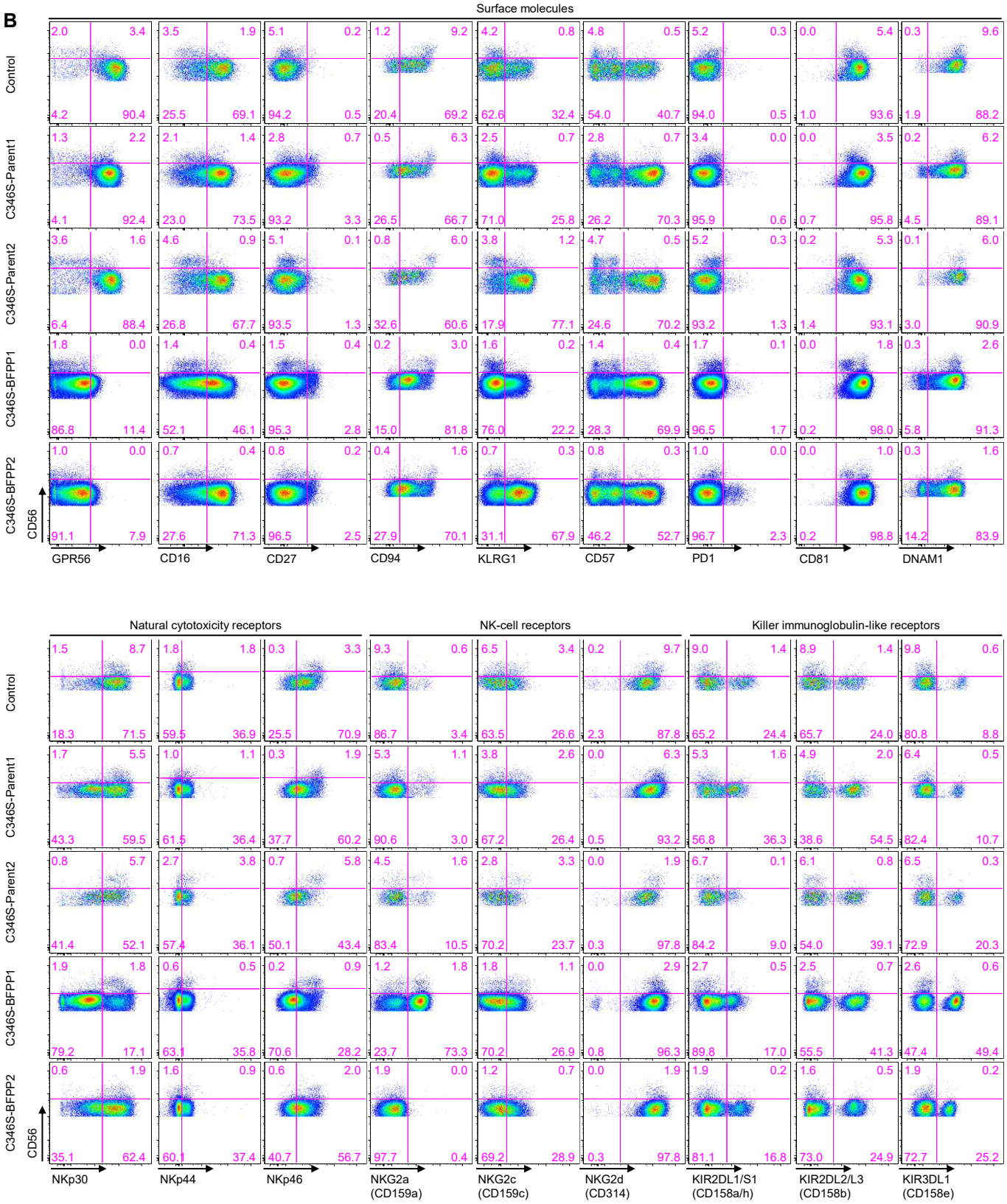

Continued on next page

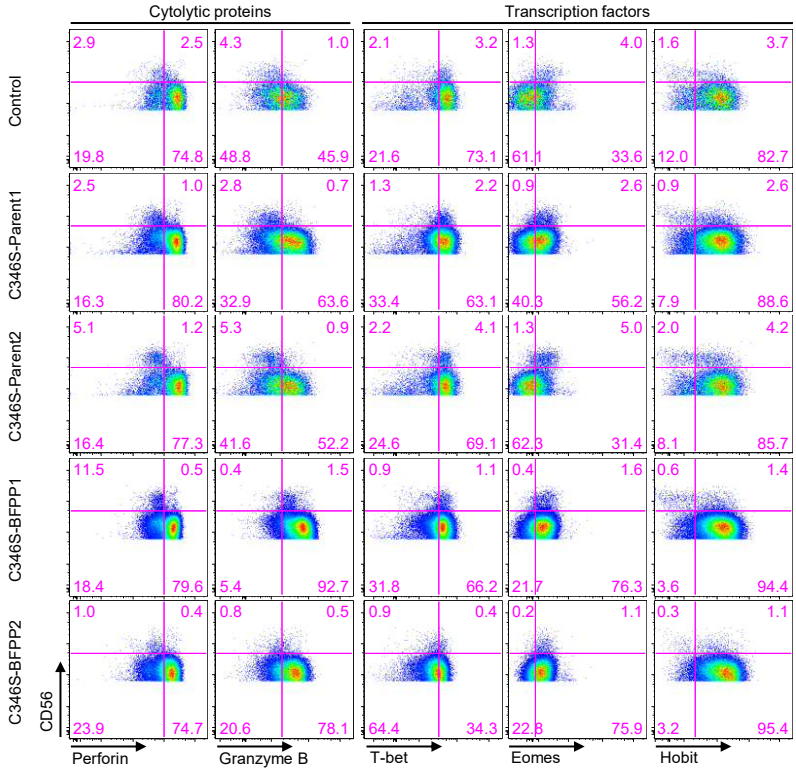

C

Cells/Molecule	Control (n=1)	C346S-Parents (n=2)	C346S-BFPP (n=2)
CD56⁺CD3⁻ NK	5.0	9.2 ± 3.7	21.7 ± 1.6
GPR56#	4251	2468 ± 265	241.0 ± 41.0
CD16#	2668	2815.5 ± 224.5	2780.0 ± 1265.0
CD27	0.5	2.4 ± 1.1	2.7 ± 0.2
CD94#	691.0	523.5 ± 32.5	560.0 ± 33.0
KLRG1	34.1	53.9 ± 27.3	45.6 ± 23.0
CD57	43.0	73.5 ± 0.6	62.2 ± 8.9
PD1	0.6	1.0 ± 0.4	2.0 ± 0.3
CD81#	3878	4639.5 ± 505.5	6119.5 ± 225.5
DNAM1	97.9	96.0 ± 0.9	89.8 ± 4.3
NKp30	79.6	54.5 ± 1.2	40.9 ± 23.1
NKp44	38.3	37.9 ± 0.7	37.3 ± 1.1
NKp46	73.5	53.9 ± 7.5	43.4 ± 14.8
NKG2a	3.8	7.3 ± 3.8	38.0 ± 37.6
NKG2c	29.5	26.8 ± 1.6	28.6 ± 0.9
NKG2d	97.4	98.8 ± 0.7	99.5 ± 0.2
KIR2DL1/S1	27.2	24.3 ± 14.7	17.4 ± 0.2
KIR2DL2/L3	26.8	50.3 ± 8.3	34.0 ± 8.6
KIR3DL1	9.8	16.6 ± 5.1	38.4 ± 12.6
Perforin#	17568	18101 ± 953	14139.5 ± 996.5
Granzyme B#	1744	2149 ± 225	4020 ± 1071
T-bet	77.2	69.6 ± 4.2	51.2 ± 16.4
Eomes	35.5	45.9 ±12.4	77.4 ± 0.5
Hobit	87.3	91.6 ± 0.2	96.5 ± 0.2

% positive cells or #geoMFI ± SEM in CD56^{dim}CD3^{-}NK

Figure S2. Expression of various surface molecules, cytolytic proteins, and transcription factors by CD56⁺CD3⁻ NK cells in BFPP patients. Related to Figure 2. (**A**) Flow-cytometric analysis of CD56⁺CD3⁻ NK cells of Dutch siblings with the R565W mutation and a control donor. (**B**) Flow-cytometric analysis of CD56⁺CD3⁻ NK cells of Palestinian siblings with the C346S mutation, their parents, and a control donors. (**C**) Quantification of (B).

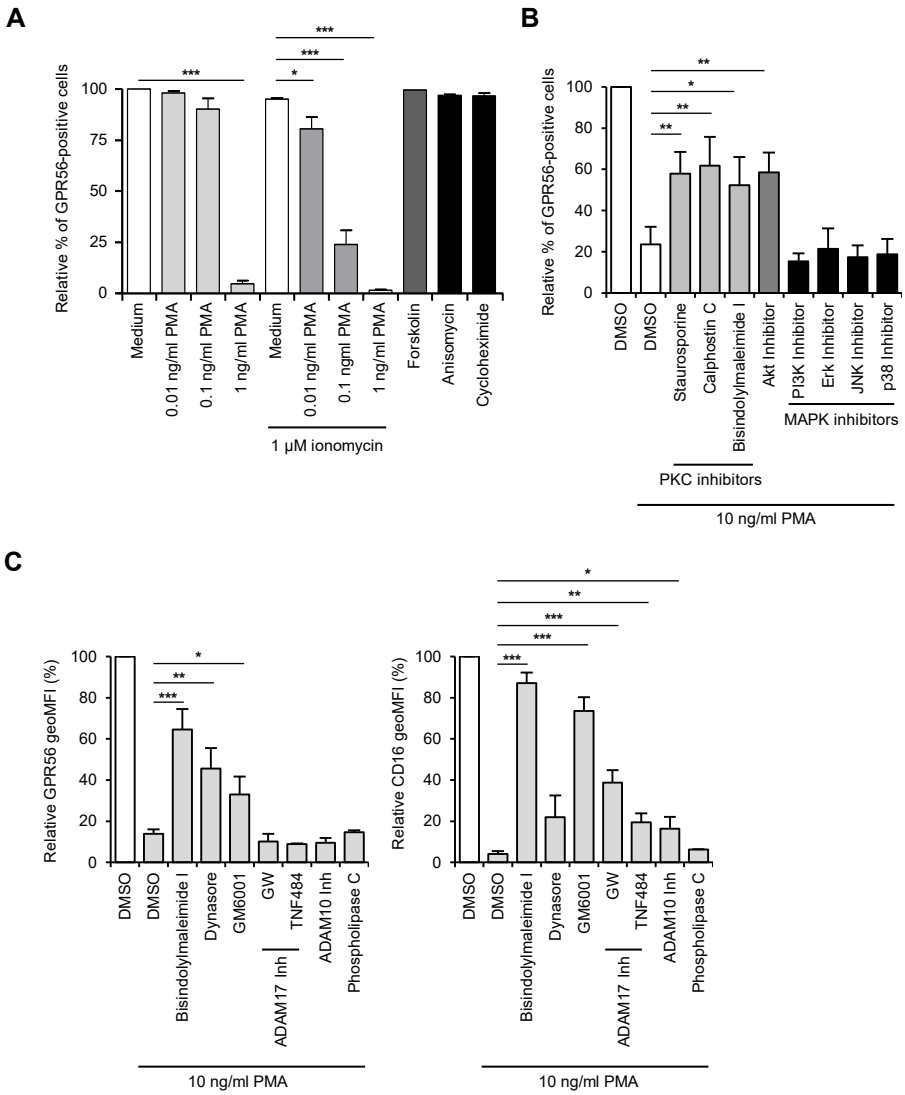

Figure S3. PKC activation induces downregulation of GPR56 in primary NK cells. Related to Figure 3. PBMCs were stimulated as indicated and analyzed by flow cytometry. (**A**) Expression of GPR56 on $CD56^{+}CD3^{-}$ NK cells incubated for 6 h with the indicated amounts of PMA, with or without 1 µM ionomycin, or with 10 µM forskolin, 10 µM anisomycin, or 3.6 µM cycloheximide. (**B**) Expression of GPR56 on $CD56^{+}CD3^{-}$ NK cells pre-treated for 30 min with PKC inhibitors (1 µM staurosporine, 1 µM calphostin C, 1 µM bisindolylmaleimide I) or with inhibitors of PKB/Akt (10 µM), PI3K (10 µM), and MAP kinases (Erk (10 µM), JNK (20 µM), and p38 (10 µM)), after which cells were incubated with 10 ng/ml PMA for 2 h. (**C**) Expression of GPR56 (left panel) and CD16 (right panel) on $CD56^{+}CD3^{-}$ NK cells pre-incubated for 1 h with inhibitors as in (A), inhibitors of ADAM17 (10 µM GW and 100 nM TNF484) and ADAM10 (10 µM), or 1 µg/ml phospholipase C in serum-free medium before incubation with PMA for 2 h. Provided are relative percentages of positive cells and geoMFIs. Data are means ± SEM of 3–5 independent experiments. *p<0.05, **p<0.01, ***p<0.005.

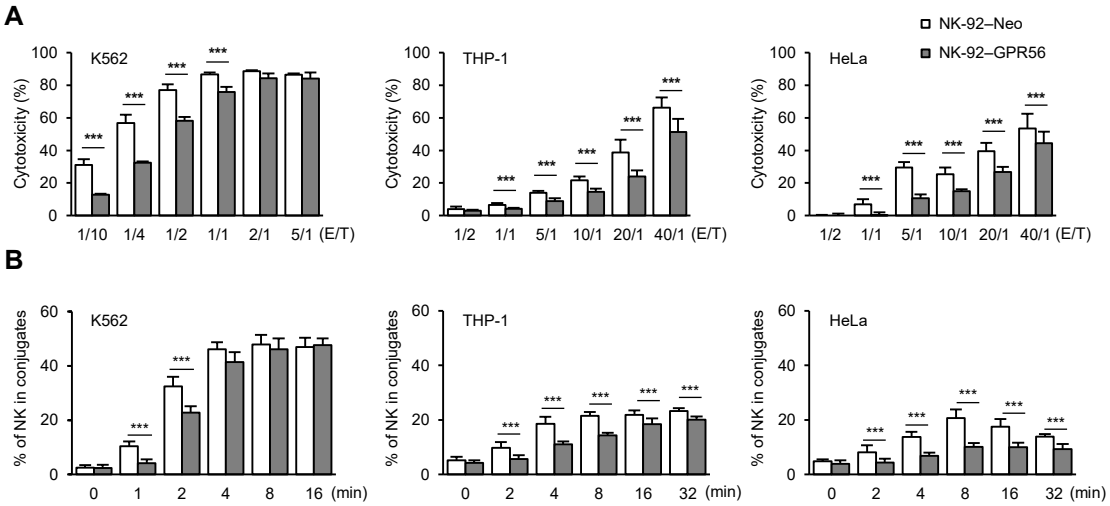

Figure S4. Forced GPR56 expression suppresses cytotoxicity and conjugation of NK-92 and target cells. Related to Figure 4. (**A**) Quantification of cytotoxic killing of K562, THP-1, and HeLa target cells by NK-92–Neo and NK-92–GPR56 cells, assessed by flow cytometry. Various E/T ratios were tested at indicated. (**B**) Quantification of cell conjugates formed between NK-92 cells and K562, THP-1, or HeLa target cells, incubated at an effector/target cell ratio of 1/2 for the indicated time periods. Fixed cells were analyzed by flow cytometry. Data are means ± SEM of 8 replicates from 4 independent experiments. ***p<0.005.

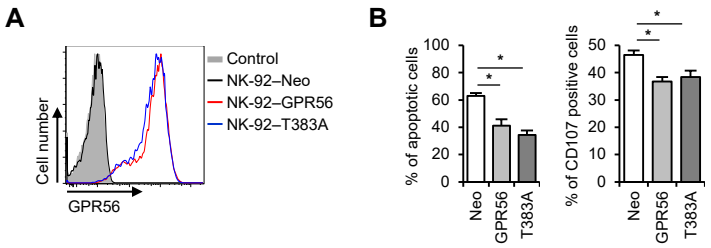

Figure S5. Suppression of cytotoxicity of NK-92 cells does not require autocatalytic processing of GPR56. Related to Figure 5. (**A**) Overexpression of wild type and cleavage-deficient GPR56 in NK-92 cells, assessed by flow cytometry. (**B**) NK-92 cells were incubated with fluorescently labeled or unlabeled K562 target cell (effector/target cell ratio=1/1) for 5 h and analyzed by flow cytometry for K562 cell death and NK-cell degranulation (CD107a). Data are means ± SEM of 3 independent experiments. *p<0.05

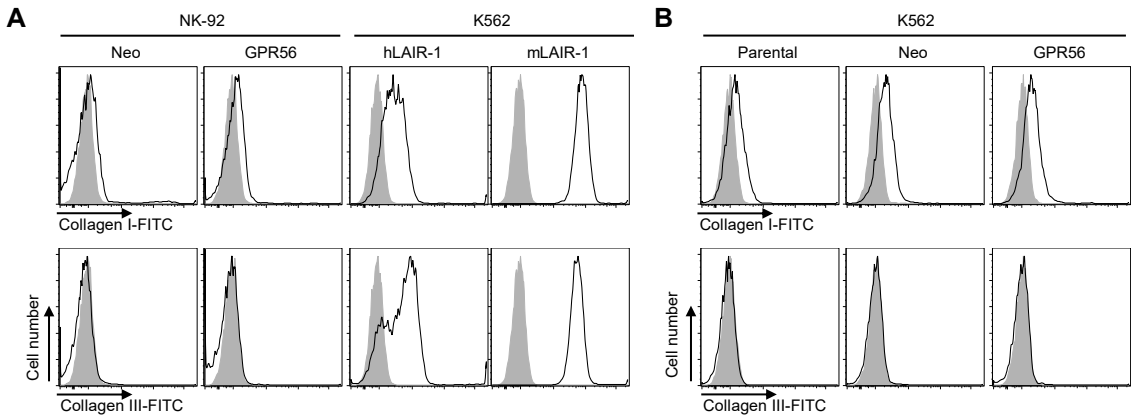

Figure S6. Collagen III does not bind GPR56 on NK-92–GPR56 cells. Related to Figure 5. (**A**,**B**) NK-92 and K562 cells overexpressing GPR56 were incubated with 10 µg/ml FITC-conjugated collagen I or III for 30 min and analyzed by flow cytometry for ligand binding. K562 cells overexpressing human (h) and mouse (m) LAIR were used to confirm collagen binding (Lebbink et al., 2006). FITC-conjugated collagen III also did not stain PBMCs (data not shown). One of three comparable experiments is shown.

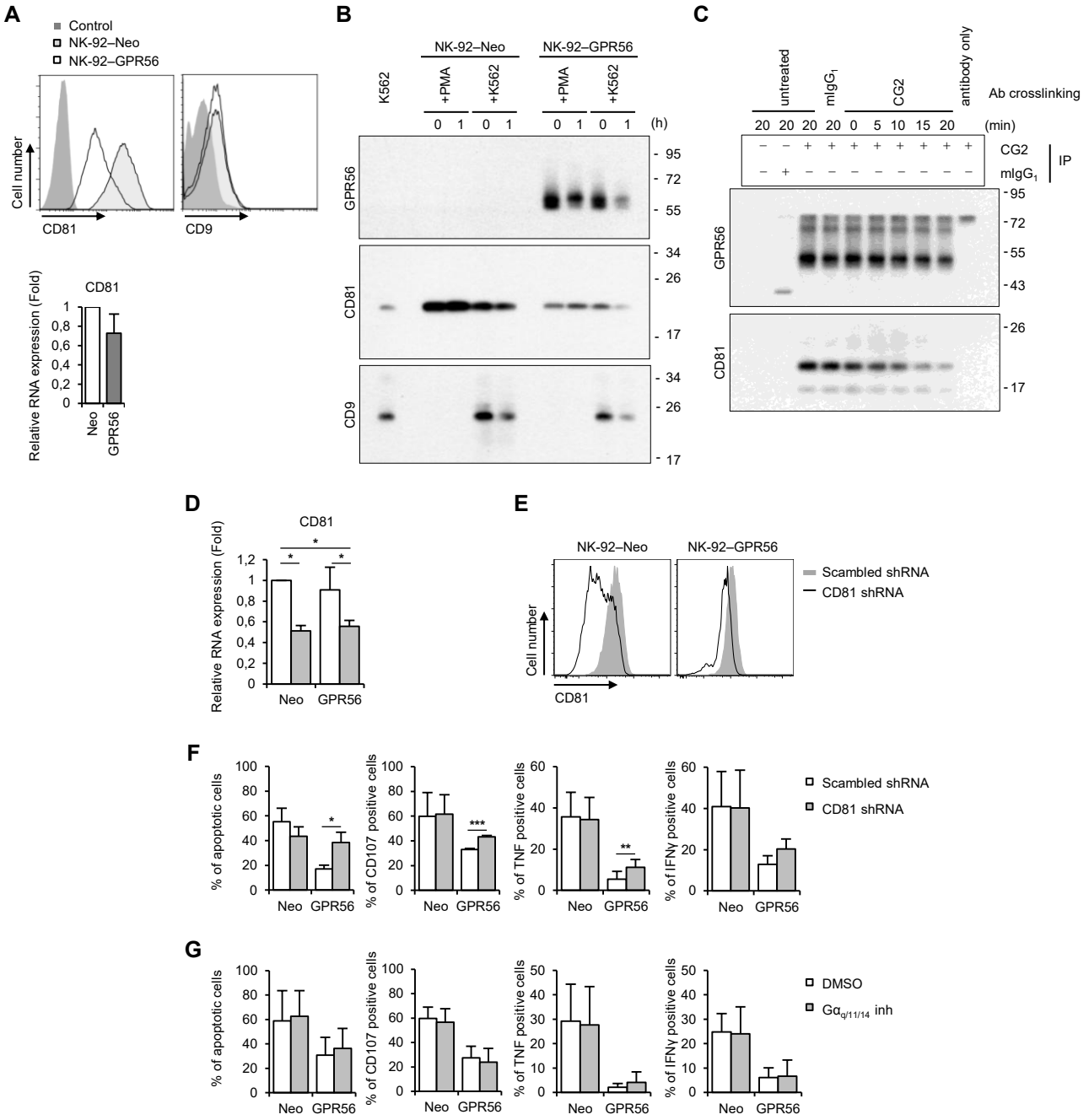

Figure S7. Molecular mechanism of GPR56 modulating effector functions in NK-92–GPR56 cells. Related to Figure 5. (**A**) Expression of CD81 and CD9 in NK-92–Neo and NK-92–GPR56 cells, analyzed by flow cytometry (left panel) and RT-PCR (right panel). (**B**) Western blot analysis of expression of GPR56, CD81, and CD9 in NK-92–Neo and NK-92–GPR56 cells. Cells were either stimulated with PMA or activated by target cells (effector/target cell ratio=1/2) for 1 h, as indicated. 1% CHAPS extract collected from 2×10^5 equivalents of K562 and 1×10^5 equivalents of NK-92 cells were loaded in each lane and analyzed by Western blotting using anti-GPR56, anti-CD81, and anti-CD9 mAbs. (**C**) NK-92–GPR56 cells were pre-treated with 10 μg/ml of CG2 for the indicated times from 0 to 20 min before lysate collection for IP using anti-GPR56 mAb CG2. Mouse IgG_1 was used as an isotype control. The presence of CD81 in each immunoprecipitate was revealed by immunoblotting. One of two comparable experiments is shown. (**D**,**E**) NK-92–Neo and NK-92–GPR56 cells, transduced with scrambled shRNA or CD81 shRNA, were analyzed by for expression of CD81. Quantification of mRNA expression by RT-PCR (D) and flow cytometry (E). (**F**) NK-92–Neo and NK-92–GPR56 cells, transduced with scrambled shRNA or CD81 shRNA, were incubated with fluorescently labeled or unlabeled K562 target cell (effector/target cell ratio=1/5) for 5 h and analyzed by flow cytometry for K562 cell death, NK-cell degranulation (CD107a), and intracellular production of TNF and IFNγ. (**G**) NK-92–Neo and NK-92–GPR56 cells, pretreated with the specific $G\alpha_{q/11/14}$ inhibitor FR900359 (1 μM) for 5 h, were incubated with fluorescently labeled or unlabeled K562 target cell (effector/target cell ratio=1/1) for 5 h and analyzed by flow cytometry for K562 cell death, NK-cell degranulation (CD107a), and intracellular production of TNF and IFNγ. Data are means ± SEM of 3-6 independent experiments. *p<0.05, **p<0.01, ***p<0.005.